Bioorganic Chemistry 84 (2019) 150–163

Contents lists available at ScienceDirect

Bioorganic Chemistry

journal homepage: www.elsevier.com/locate/bioorg

1,3,4-oxadiazole/chalcone hybrids: Design, synthesis, and inhibition of leukemia cell growth and EGFR, Src, IL-6 and STAT3 activities

Marwa Ali A. Fathi[a,1], Amer Ali Abd El-Hafeez[b,c,d,1,*], Dalia Abdelhamid[a], Samar H. Abbas[a,*], Monica M. Montano[d], Mohamed Abdel-Aziz[a]

[a] Medicinal Chemistry Department, Faculty of Pharmacy, Minia University, Minia 61519, Egypt
[b] Pharmacology and Experimental Oncology Unit, Cancer Biology Department, National Cancer Institute, Cairo University, Cairo 11796, Egypt
[c] Pharmacotherapy Department, Graduate School of Biomedical and Health Sciences, Hiroshima University, Hiroshima 734-8553, Japan
[d] Pharmacology Department, Case Western Reserve University School of Medicine, 10900 Euclid Avenue, Cleveland, OH 44106, USA

ARTICLE INFO

Keywords:
Leukemia
Oxadiazole
Chalcone
Tyrosine kinases
Cytokines
STAT3

ABSTRACT

A new series of 1,3,4-oxadiazole/chalcone hybrids was designed, synthesized, identified with different spectroscopic techniques and biologically evaluated as inhibitors of EGFR, Src, and IL-6. The synthesized compounds showed promising anticancer activity, particularly against leukemia, with **8v** being the most potent. The synthesized compounds exhibited strong to moderate cytotoxic activities against K-562, KG-1a, and Jurkat leukemia cell lines in MTT assays. Compound **8v** showed the strongest cytotoxic activity with IC_{50} of 1.95 μM, 2.36 μM and 3.45 μM against K-562, Jurkat and KG-1a leukemia cell lines, respectively. Moreover; the synthesized compounds inhibited EGFR, Src, and IL-6. Compound **8v** was most effective at inhibiting EGFR (IC_{50} = 0.24 μM), Src (IC_{50} = 0.96 μM), and IL-6 (% of control = 20%). Additionally, most of the compounds decreased STAT3 activation.

1. Introduction

Leukemia is a type of cancer that starts in the blood-forming cells of the bone marrow [1]. Chemotherapeutic agents are found to be effective in killing leukemic cells, however, the 5-year overall survival is very poor [2]. Most patients relapse by tumor regrowth are initiated by chemoresistant leukemia cells. Potential bases for therapeutic resistance in leukemia treatment have been reported [3–5]. The signal transducers and activators of transcription 3 (STAT3) is a critical signaling intermediate in leukemia cells. STAT3 can be activated *via* phosphorylation by tyrosine kinases such as EGFR and Src and cytokines such as IL-6 [6]. The activation of STAT3 in leukemia is associated with poor prognosis [7]. Furthermore, development of chemo-resistant leukemic cells has been attributed to activation of the STAT3 pathway [8–11]. Consequently, significant effort has been committed towards the development of drugs that target STAT3 activators, and includes gefitinib (EGFR inhibitor) [12], dasatinib (Src inhibitor) [13] and tocilizumab (IL-6 inhibitor) [14,15]. Unfortunately, the targeting of STAT3 activators such as EGFR, Src or IL-6 individually resulted only in moderate clinical efficacy [16–18]. Moreover, resistance develops due to the cross-talk between the pathways that activates STAT3, thus bypassing the inhibition of any one of the activators [8,19–21]. Recently, efforts have shifted toward the generation of drug candidates that can target two STAT3 activators. For example, Lin et al. [22] synthesized oxazolo[4,5-*g*]quinazolin-2(1*H*)-ones derivatives as dual EGFR and Src inhibitors. Additionally, a series of azaacridine derivatives were synthesized as dual EGFR and Src inhibitors [23]. These dual EGFR and Src inhibitors have the potential to overcome the resistance of leukemia cells to STAT3 inhibition. However, STAT3 activation could occur *via* pathways other than EGFR and Src, such as IL-6 [24–26]. Dual EGFR and Src inhibition may not be sufficient for sustained inhibition of STAT3 activation. Therefore, the development of drugs that target EGFR, Src, and IL-6 may offer a therapeutic advantage.

Oxadiazole derivatives are typical heterocyclic compounds that have exhibited potential as anticancer therapeutics [27–32]. The anticancer activities of 1,3,4-oxadiazole involve different mechanisms, and included inhibition of matrix metalloproteinase-9 [33], tubulin polymerization [34], growth factors [30], NF-κB signaling [35], Bcl-2 [36], cell cycle progression at G2/M phase [37], thymidine phosphorylase [38,39], and STAT3 [40–44]. The potential antitumor effects of

* Corresponding authors at: Medicinal Chemistry Department, Faculty of Pharmacy, Minia University, Minia 61519, Egypt (S.H. Abbas). Pharmacology and Experimental Oncology Unit, Cancer Biology Department, National Cancer Institute, Cairo University, Cairo 11796, Egypt (A.A. Abd El-Hafeez).
E-mail addresses: amer.ali@nci.cu.edu.eg (A.A. Abd El-Hafeez), samar_hafez@mu.edu.eg (S.H. Abbas).
[1] Both authors contributed equally to this work.

https://doi.org/10.1016/j.bioorg.2018.11.032
Received 24 July 2018; Received in revised form 19 November 2018; Accepted 20 November 2018
Available online 22 November 2018
0045-2068/

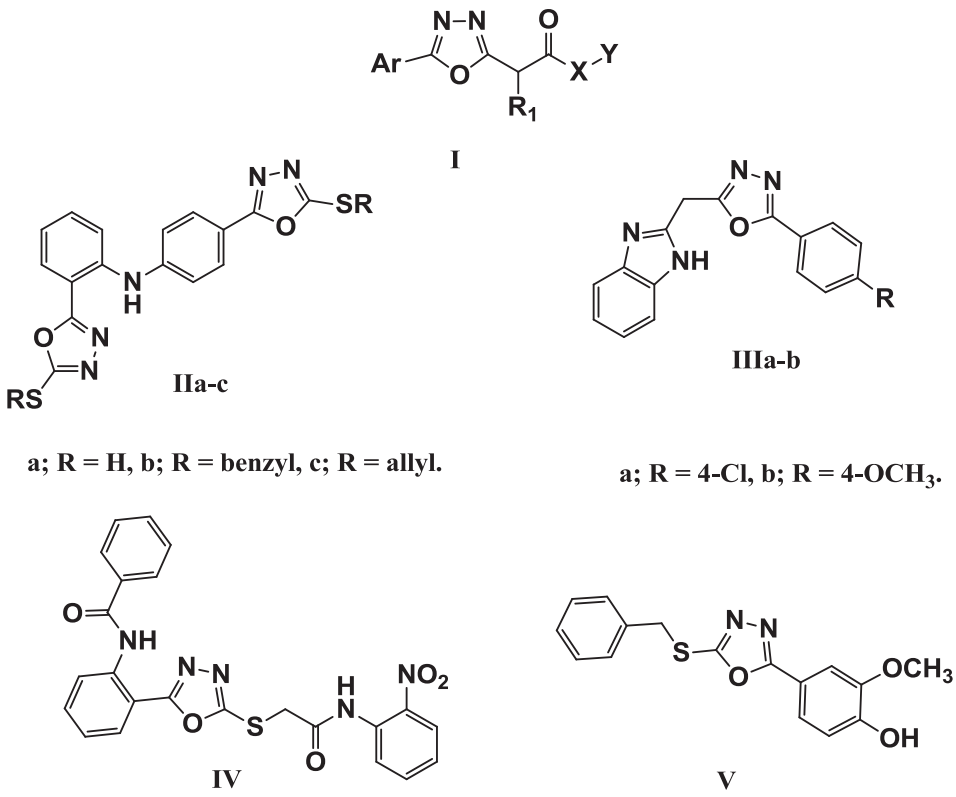

Fig. 1. Structures of Compounds **I-V.**

oxadiazole derivatives occur mainly *via* the inhibition of STAT3 pathways directly [40] or indirectly [41–44]. A library of 1,3,4-oxadiazole-2-carboxamide compounds was registered in a U.S. patent with the general formula **I** (Fig. 1). These compounds inhibited STAT3 at a concentration of 100 μM, as well as inhibited growth of several cancer cell lines, including MDA-MB-468 and human lymphoma cells (SCC-3) [45]. The 2, 4′-bis mercapto-1,3,4-oxadiazole diphenylamine derivative **IIa-c** (Fig. 1) showed more potent anticancer activity with IC_{50} less than or equal to 2 μM and inhibited EGFR tyrosine kinase activity [41]. The 1,3,4-oxadiazole linked benzimidazole derivative **III a-b** inhibited the EGFR receptor at 0.081 and 0.098 μM, and were more cytotoxic than 5-fluorouracil [42]. The 1,3,4-oxadiazole-2-thione derivative **IV** was the most potent Src kinase inhibitor among 384 tested compounds, with IC_{50} equal to 1.9 μM [44]. The 1,3,4-oxadiazole derivative **V** was also effective in inhibiting the release of IL-1, IL-6 and IL-10 in ConA-stimulated mouse lymph node cells [43].

On the other hand, chalcones are precursors of flavonoids and isoflavonoids that exhibited anti-cancer activities, which may be attributed to the inhibition of different molecular targets [46] including EGFR [47,48], Src family protein [49], IL-6 [50], and others [51]. For example, caspase-3 levels were significantly increased while STAT3 levels were decreased in the leukemia HL60 cell line upon treatment with chalcones **VIa-b (**Fig. 2**)** [52]. Additionally, Butein **VII** (Fig. 2) exerted anticancer effects in human hepatocellular carcinoma through suppression of constitutive and IL-6-induced STAT3 activation, as well as the inhibition of c-Src, JAK1, and JAK2 activation [53]. Moreover, Cardomin **VIII** (Fig. 2) exhibited significant anticancer effects in prostate cancer by suppression of STAT3 phosphorylation, nuclear translocation, DNA binding ability, and inhibition of STAT3 dimerization. Computational modeling indicated that Cardomin **VIII** can bind to the Src Homology 2 domain [54]. Several chalcones were derivatized with different bioactive heterocyclic moieties with the goal of generating anticancer agents with increased selectivity, ability to overcome drug resistance, and decreased side effects. 1,2,4-Triazole/chalcone hybrid **IX** (Fig. 2) induced caspase-3 dependent apoptosis in A549 cells through both extrinsic and intrinsic pathways [51]. Additionally, pyrazolo[1,5-*a*]pyrimidine/chalcone hybrid **X** showed (Fig. 2) promising anti-proliferative activity and downregulated EGFR, p-EGFR, STAT3, and p-STAT3 in MDA-MB-231 cells [55]. Moreover; benzo[*c*]furan-chalcone derivative **XI** (Fig. 2) exhibited significant cytotoxicity in MCF-7 cell lines *via* inhibition of tubulin polymerization ($IC_{50} = 5.51 \times 10^{-5}$ μM) and EGFR-TK phosphorylation ($IC_{50} = 0.09$ μM) [56]. The triazoloquinoxaline-chalcone hybrids **XIIa-b** also inhibited EGFR-TK in the submicromolar range (0.039 to 0.083 μM) [57]. Benzimidazole/ chalcone hybrids **XIIIa-b** (Fig. 2) are EGFR antagonist that exhibited promising cytotoxicity against the HCT116 and H460 cell lines with IC_{50} ranging from 6.83 to 12.52 μM [58].

Based on the studies discussed above, the present study involved the design and synthesis of a series of 1,3,4-oxadiazole/chalcone hybrids (Fig. 3) with the combined abilities to inhibit EGFR, Src, and IL-6. The hybrids were designed such that the oxadiazole or chalcone moieties possess a methoxy group (*s*) or chlorine as electron donating or as electron withdrawing substituents; respectively. The synthesized compounds were evaluated for their cytotoxic activities against different cancer cell lines, including three different leukemia cell lines (K-562, KG-1a, and Jurkat). Moreover, their inhibitory activities against EGFR, Src, IL-6, and STAT3 were evaluated.

2. Results and discussion

2.1. Chemistry

The target compounds and intermediates were prepared as outlined in Scheme 1.

Alkylation of oxadiazole derivatives **4a-e** with acetylated chalcone derivatives **7a–e** was achieved in acetonitrile in the presence of TEA to generate the target compounds **8a-x** in a good yield ranging from 51% to 89% [59]. ^{1}H NMR and ^{13}C NMR confirmed the formation of target compounds. ^{1}H NMR spectra of compounds **8a-x** showed a singlet

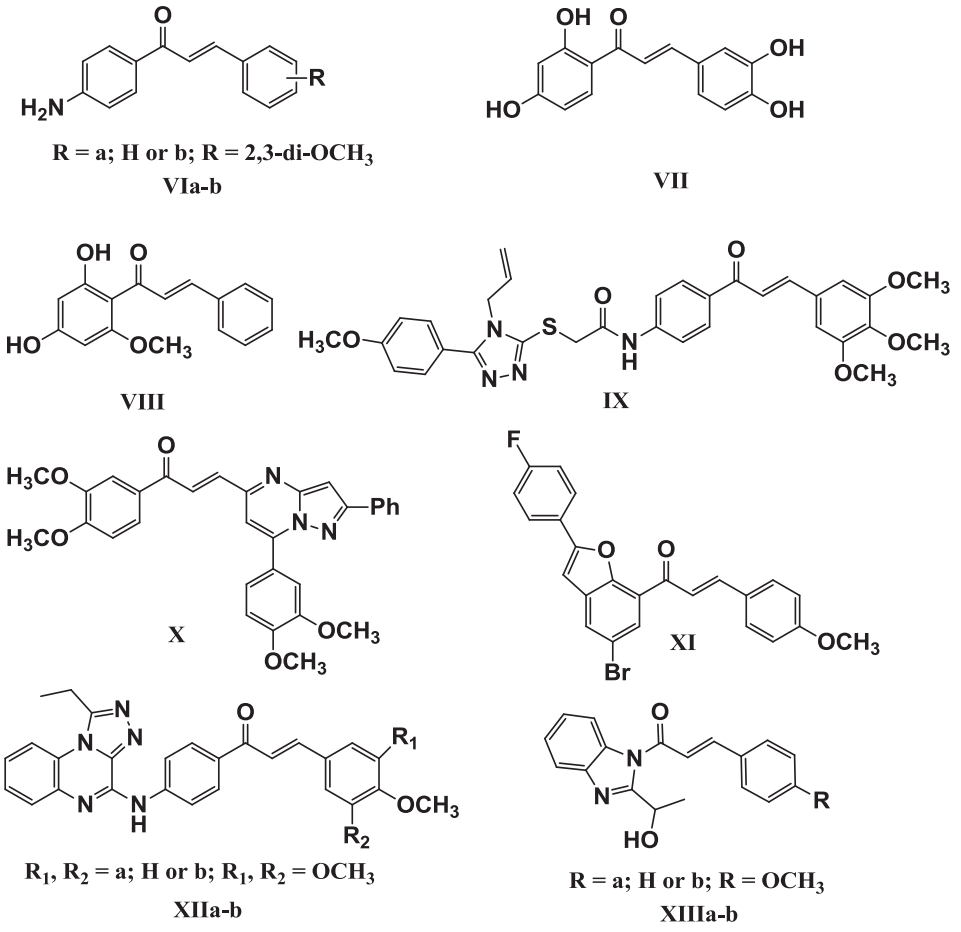

Fig. 2. Structures of compounds **VI-XIII**.

signal at δ: 4.09–4.80 ppm related to (S-CH_2-CO). Furthermore, the two chalcone protons appear at the aromatic region as doublet signals at δ: 7.81–7.98 ppm and 7.39–7.78 ppm with coupling constant J = 15.00–16.00 Hz. The amide proton NH appears as singlet signals at δ 9.74–11.25 ppm. The ^{13}C NMR spectra of compounds **8a-x** revealed the presence of two carbonyl groups appearing at δ: 187.89–189.05 ppm and δ: 166.02–169.22 ppm related to C═O of chalcone and *N*–C═O, and a characteristic signal of SCH_2 appears at 36.31–37.43 ppm.

2.2. Biological evaluation

2.2.1. Cytotoxic assays

2.2.1.1. In vitro one dose anticancer assay. All the twenty-four synthesized compounds (**8a-x)** were selected by the National Cancer Institute (NCI), USA for *in vitro* anticancer screening. Compounds were screened at 10 μM dose using the Sulforhodamine B colorimetric assay against the full NCI panel of 60 cell lines consisting of nine tumor subpanels, which include leukemia, lung, colon, melanoma, renal,

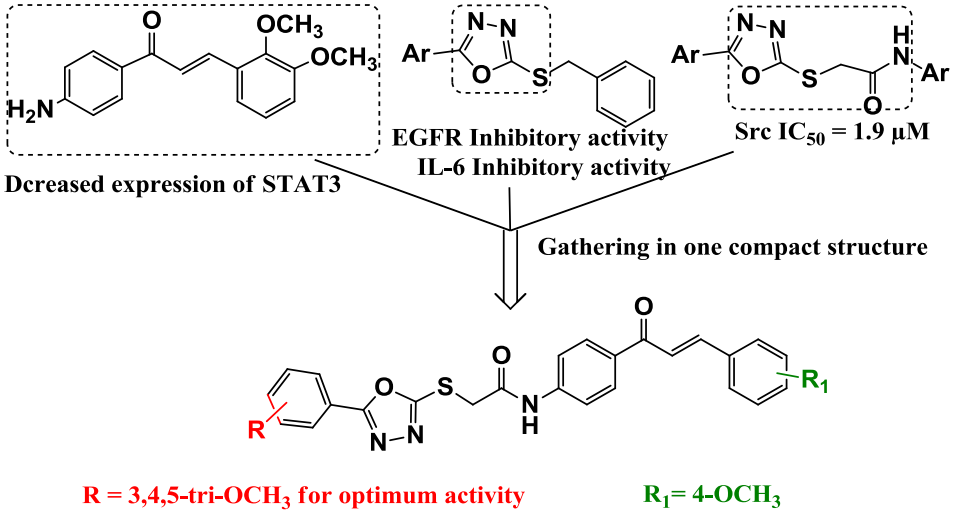

Fig. 3. Pharmacophore of the target compounds.

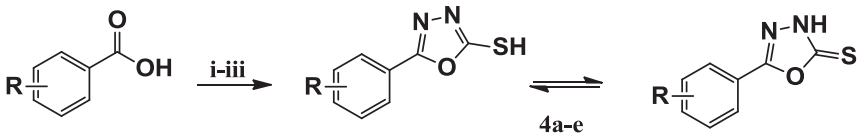

R : a) H, b) 4-Cl, c) 4-OCH_3, d) 3,4-Di-OCH_3, e) 3,4,5-Tri-OCH_3.

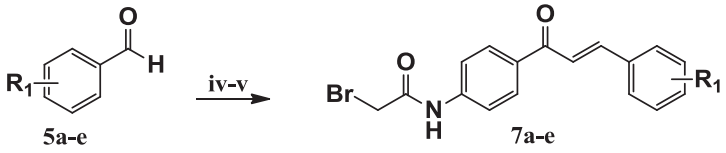

R_1 : a) H, b) 4-Cl, c) 4-OCH_3, d) 3,4-Di-OCH_3, e) 3,4,5-Tri-OCH_3.

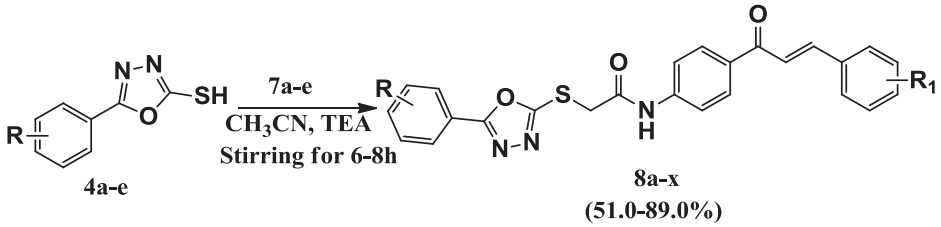

Compd.	R	R_1	Compd.	R	R_1
8a	H	H	**8m**	4-OCH_3	3,4-di-OCH_3
8b	H	4-Cl	**8n**	4-OCH_3	3,4,5-tri-OCH_3
8c	H	3,4-di-OCH_3	**8o**	3,4-di-OCH_3	H
8d	H	3,4,5-tri-OCH_3	**8p**	3,4-di-OCH_3	4-Cl
8e	4-Cl	H	**8q**	3,4-di-OCH_3	4-OCH_3
8f	4-Cl	4-Cl	**8r**	3,4-di-OCH_3	3,4-di-OCH_3
8g	4-Cl	4-OCH_3	**8s**	3,4-di-OCH_3	3,4,5-tri-OCH_3
8h	4-Cl	3,4-di-OCH_3	**8t**	3,4,5-tri-OCH_3	H
8i	4-Cl	3,4,5-tri-OCH_3	**8u**	3,4,5-tri-OCH_3	4-Cl
8j	4-OCH_3	H	**8v**	3,4,5-tri-OCH_3	4-OCH_3
8k	4-OCH_3	4-Cl	**8w**	3,4,5-tri-OCH_3	3,4-di-OCH_3
8l	4-OCH_3	4-OCH_3	**8x**	3,4,5-tri-OCH_3	3,4,5-tri-OCH_3

i) EtOH, Conc H_2SO_4, reflux for 12-18 h. (75.7-87.2 %). ii) $NH_2NH_2H_2O$ (97%), EtOH, reflux 5-8 h, (72.7-80.2 %). iii) 1- CS_2, KOH, EtOH, reflux 12 h.; 2- Conc HCl, (60.0-87.0%). iv) *p*-aminoacetophenone, KOH (60%), EtOH, Stirring 4 h, (67.3-82.9%). v) $BrCH_2COBr$, CH_2Cl_2, K_2CO_3, H_2O, Stirring overnight, (69.7-78%).

Scheme 1. Synthesis of the target compounds **8a-x**.

prostate, CNS, ovarian, and breast cancer cell lines.

The compounds tested exhibited promising anticancer activities (Table 1 and 2 **supporting information**) against human cancer cells, particularly leukemia cell lines. Among the synthesized compounds, **8a**, **8n**, **8p**, and **8v** were the most potent (Mean growth inhibition % = 37.77, 27.29, 28.20, and 132.29; respectively).

Compound **8v** exhibited potent cytotoxicities against most of the tested cell lines, with complete cell death observed for 45 used cell lines and % growth inhibition ranging from 101.51 to 191.80% (Table 2 **supporting information**).

Six compounds, **8a, 8d, 8m, 8n, 8s,** and **8v** exhibited significant anticancer activity against K-562 cell line with % growth inhibition ranging from 35.80 to 152.18%. Additionally; compounds **8a**, **8d**, **8e**, **8j**, **8k-n**, **8p**, **8s**, **8v**, and **8x** showed anticancer activity against RPMI-8226 cell line with % growth inhibition ranging from 31.29 to 143.74%. Compounds **8a**, **8d**, **8e**, **8i-k, 8m**, **8n**, **8p**, **8s**, **8v** and **8x** exhibited good anticancer activity against SR cell line with % growth inhibition ranging from 32.85 to 160.49%.

On the other hand, compounds **8a**, **8d, 8 l-n,** and **8p** exhibited only moderate anticancer activity against MOLT-4 cell line with % growth

Table 1
GI_{50} and TGI of compound **8v** against the panel of 58 cell lines representing 9 different cancers tested using NCI's *in vitro* five dose anticancer assay.

Panel/Cell Line	GI_{50} (μM)	TGI (μM)	Panel/Cell Line	GI_{50} (μM)	TGI (μM)
Leukemia			Melanoma		
CCRF-CEM	1.84	4.56	LOX IMVI	0.32	1.28
HL-60(TB)	2.00	4.10	MALME-3M	1.68	3.45
MOLT-4	2.05	5.27	M14	1.60	3.30
RPMI-8226	1.73	4.31	MDA-MB-435	1.70	3.40
SR	1.86	4.01	SK-MEL-2	1.79	4.82
Non-Small Cell Lung Cancer			SK-MEL-28	1.74	3.40
A549/ATCC	1.84	3.53	SK-MEL-5	2.14	5.24
EKVX	1.79	3.98	UACC-257	2.16	4.69
HOP-62	2.13	4.53	UACC-62	1.73	3.43
HOP-92	1.93	4.23	Ovarian Cancer		
NCI-H226	2.67	5.69	IGROV1	1.54	3.75
NCI-H23	1.88	3.97	OVCAR-3	1.78	3.38
NCI-H322M	1.59	2.98	OVCAR-4	2.00	4.62
NCI-H460	2.00	3.85	OVCAR-5	1.72	3.30
NCI-H522	1.55	3.21	OVCAR-8	2.32	5.73
Colon Cancer			NCI/ADR-RES	2.42	7.03
COLO 205	1.94	3.84	SK-OV-3	2.42	5.68
HCC-2998	1.88	3.65	Renal Cancer		
HCT-116	0.50	1.94	786–0	1.70	3.36
HCT-15	1.63	3.22	A498	11.00	23.60
HT29	1.83	3.62	ACHN	1.72	3.22
KM12	1.77	3.40	RXF 393	1.74	3.54
SW-620	1.86	3.60	SN12C	1.83	3.57
CNS cancer			TK-10	1.52	3.03
SF-268	1.79	3.96	UO-31	1.46	2.97
SF-295	1.77	3.35	Breast cancer		
SF-539	1.64	3.03	MCF7	1.27	3.68
SNB-19	1.78	3.56	MDA-MB231/ATCC	1.82	3.50
SNB-75	1.47	3.15	HS 578T	2.65	7.76
U251	1.68	3.18	BT-549	1.40	2.81
Prostate Cancer			T-47D	2.05	5.08
PC-3	1.75	3.30	MDA-MB-468	2.10	5.02
DU-145	1.75	3.21			

inhibition ranging from 31.88 to 108.34%.

2.2.1.2. In vitro five-dose anticancer assay. Compound **8v** was selected for advanced five-dose testing against the full panel of 58 human tumor cell lines. All of the 58 cell lines, representing nine tumor subpanels, were incubated at five different concentrations of (0.01, 0.1, 1, 10 and 100 μM). The data indicate that compound **8v** exhibited broad-spectrum antitumor activity with GI_{50} ranging from 0.32 to 11 μM, with selectivity ratio ranging between 0.65 and 1.20 at GI_{50} level (Table 1). Moreover, compound **8v** showed the ability to inhibit growth of all the cell lines tested, with TGI concentration ranging from 1.28 to 23.60 μM. Compound **8v** exhibited LC_{50} with concentrations ranging from 5.28 to > 100 μM.

2.2.1.3. In vitro anti-proliferative assay using K-562, KG-1a, and Jurkat cells. The cytotoxic activities of the synthesized compounds were determined using three different leukemia cell lines (K-562, KG-1a, and Jurkat) and evaluated using MTT assays. Results presented in Table 2 indicate that most of the synthesized 1,3,4-oxadiazole/chalcone derivatives exhibited strong to moderate cytotoxic activities against the three leukemia cell lines. The relative sensitivities of leukemia cells toward the synthesized compounds were K-562 > Jurkat > KG-1a. Consistent with the NCI results, **8v** showed the strongest cytotoxic activity among the derivatives synthesized, with the relative sensitivities of K-562 (IC_{50} = 1.95 μM) > Jurkat (IC_{50} = 2.36 μM) > KG-1a (IC_{50} = 3.45 μM).

Our structure-activity relationship (SAR) analyses indicate that the type of substitution in both phenyl rings is essential for anticancer activity. For anticancer activity, the substitution of phenyl ring carrying the oxadiazole moiety should be either H, *p*-methoxy or 3,4,5-trimethoxy group (s), with an effective substitution order of 3,4,5-trimethoxy groups > H > *p*-methoxy group. Also, the more effective substitutions of the chalcone phenyl ring are either H, *p*-methoxy or 3,4,5-trimethoxy group (s). For optimal activity, R must be 3,4,5-trimethoxy groups and R_1 must be methoxy group in *p*-position. Thus for good anti-cancer activity, the two phenyl rings should be either unsubstituted or one of the rings should carry *p*-methoxy group, while the second ring should contain 3,4,5-trimethoxy groups.

Table 2
Cytotoxic activity of oxadiazole/chalcone hybrids, **8a-x**, against three leukemia cell lines.

Compound	(IC_{50} μM) ± SD		
	K-562	**KG-1a**	**Jurkat**
8a	7.21 ± 0.35	8.85 ± 0.22	8.47 ± 1.03
8b	75.35 ± 4.61	82.24 ± 4.56	78.71 ± 2.13
8c	69.54 ± 5.15	95.22 ± 3.88	75.22 ± 1.25
8d	22.84 ± 1.32	31.34 ± 1.05	28.28 ± 0.62
8e	93.31 ± 5.21	> 100	> 100
8f	82.27 ± 3.08	91.54 ± 4.15	88.61 ± 1.35
8g	13.05 ± 1.65	55.64 ± 1.34	41.21 ± 0.91
8 h	72.14 ± 3.32	84.64 ± 5.21	78.06 ± 2.10
8i	55.34 ± 4.89	78.95 ± 3.02	62.56 ± 1.37
8j	22.61 ± 2.34	25.22 ± 0.48	31.13 ± 0.46
8k	58.42 ± 3.75	71.07 ± 1.22	62.67 ± 2.71
8 l	35.22 ± 2.05	38.32 ± 2.45	33.28 ± 1.22
8 m	23.11 ± 0.28	31.54 ± 0.42	28.36 ± 0.85
8*n*	10.25 ± 0.94	15.97 ± 0.96	13.15 ± 0.08
8o	58.37 ± 5.45	65.64 ± 2.31	94.09 ± 5.31
8p	16.09 ± 1.08	22.52 ± 1.07	17.24 ± 0.79
8q	40.22 ± 2.82	45.29 ± 2.31	31.94 ± 1.30
8r	> 100	93.08 ± 1.14	> 100
8s	15.14 ± 0.25	32.12 ± 0.64	25.14 ± 0.45
8 t	73.25 ± 3.72	84.57 ± 1.28	76.36 ± 1.31
8u	84.22 ± 4.36	95.69 ± 2.48	> 100
8v	1.95 ± 0.18	3.45 ± 0.25	2.36 ± 0.47
8w	90.34 ± 2.91	> 100	> 100
8x	62.15 ± 3.07	71.48 ± 1.18	69.17 ± 0.15
Cisplatin	3.21 ± 0.45	12.15 ± 3.41	15.12 ± 1.35

2.2.2. 1,3,4-oxadiazole/chalcone hybrids inhibited EGFR and Src kinase activities and protein expression

The oxadiazole/chalcone hybrids **8a-x** inhibited EGFR kinase activity with relatively lower concentrations than that required for the inhibition of Src Kinase activity. The effects of synthesized compounds on EGFR and Src tyrosine kinases are presented in Table 3. Compounds **8a**, **8n** and **8v** displayed the highest inhibitory activities against EGFR (IC_{50} = 0.24–2.35 μM) as well as Src (IC_{50} = 0.96–6.24 μM). While compounds **8b**, **8g-8m**, **8p**, **8q**, **8s**, **8 t**, and **8x** exhibited moderate inhibitory activities against EGFR (IC_{50} = 10.24–35.15 μM) and Src (IC_{50} = 12.5–44.1 μM). On the other hand, compounds **8c**, **8e**, **8f**, **8o**, **8r**, **8u**, and **8w** showed the lowest activity against EGFR (IC_{50} = 48.34–71.15 μM) and Src (IC_{50} = 50.32–76.2 μM).

To confirm the ability of the synthesized compounds to inhibit EGFR and Src, we evaluated the effects of the most potent compound **8v**, on the expression levels of EGFR, p-EGFR, Src and p-Src in K562 cells using Western blot analysis. As shown in Fig. 4, compound **8v** downregulated the protein expression levels of p-EGFR, EGFR, p-Src and Src in a dose-dependent manner. Therefore, it was reasonable to conclude that the anti-proliferative effect of compound **8v** may be attributed to the inhibition of EGFR and Src.

Table 3
EGFR and Src kinases inhibitory activity of 1,3,4-oxadiazole/chalcone hybrids.

Compound	EGFR (IC_{50} μM)	Src (IC_{50} μM)	Compound	EGFR (IC_{50} μM)	Src (IC_{50} μM)
8a	1.23 ± 0.25	4.5 ± 1.2	**8n**	2.35 ± 0.95	6.24 ± 0.86
8b	35.15 ± 1.36	44.1 ± 3.5	**8o**	71.15 ± 3.25	51.24 ± 5.6
8c	64.35 ± 3.56	57.3 ± 2.4	**8p**	13.26 ± 0.65	13.67 ± 0.89
8d	11.22 ± 1.25	13.41 ± 1.6	**8q**	11.38 ± 1.54	29.48 ± 1.23
8e	59.35 ± 5.63	74.4 ± 3.6	**8r**	63.25 ± 2.36	76.2 ± 3.65
8f	64.68 ± 3.65	50.32 ± 3.5	**8s**	12.35 ± 0.8	15.34 ± 1.25
8g	12.67 ± 1.25	22.14 ± 2.15	**8t**	22.34 ± 2.35	40.21 ± 1.34
8h	30.25 ± 2.35	41.36 ± 4.5	**8u**	55.45 ± 4.35	53.09 ± 5.6
8i	29.34 ± 3.65	43.67 ± 3.5	**8v**	0.24 ± 0.035	0.96 ± 0.2
8j	11.47 ± 1.24	25.34 ± 1.56	**8w**	48.34 ± 2.36	60.34 ± 2.5
8k	18.34 ± 2.35	33.64 ± 2.35	**8x**	20.5 ± 1.35	35.12 ± 3.26
8l	12.34 ± 1.35	24.98 ± 3.46	**Dasatinib**	0.8 ± 0.23	< 0.001
8m	10.24 ± 0.36	12.5 ± 0.3	**Gefitinib**	0.023 ± 0.004	1.25 ± 0.15

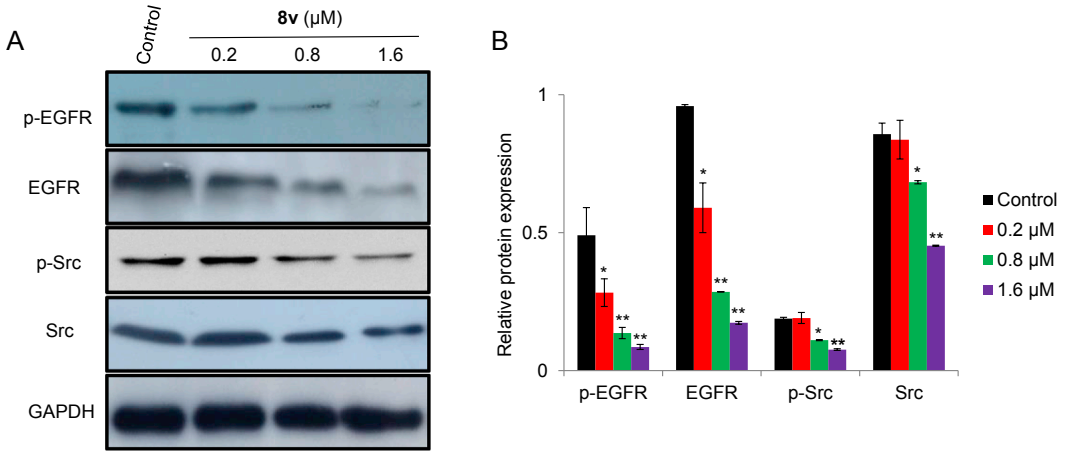

Fig. 4. (A) Western blotting analysis of the expression of EGFR, p-EGFR, Src and p-Src in K562 cells treated with 0, 0.2, 0.8, or 1.6 μM oxadiazole chalcone hybrid **8v**. GAPDH served as a loading control. **(B)** The protein expression of EGFR, p-EGFR, Src and p-Src after treatment with different concentrations of compound **8v**. The values are expressed as the mean ± SD based on three different experiments. *, P < 0.05 and **, P < 0.005 indicate a significant difference compared with vehicle treated cells.

2.2.3. 1,3,4-Oxadiazole/chalcone hybrids inhibited IL-6 production

K562 cells were treated with 10 μM of 1,3,4-oxadiazole/chalcone hybrids **8a-x** for 24 h, after which media were collected to determine IL-6 protein levels. As illustrated in Fig. 5**A, 1**,3,4-oxadiazole/chalcone hybrids decreased IL-6 protein levels. Consistent with relative effectiveness of the compounds in downregulating EGFR and Src, compounds **8a**, **8n**, and **8v** were found to be most effective at downregulating IL-6 levels (% of control = 20–23%). Compounds, **8b**, **8g-8m**, **8p**, **8q**, **8s**, **8 t**, and **8x** induced moderate inhibition of IL-6 levels (% of control = 30–75%). On the other hand, compounds **8c**, **8e**, **8f**, **8o**, **8r**, **8u**, and **8w** did not significantly downregulate IL-6 levels (% of control = 82–98%). The initial downregulation of the levels of IL-6 protein were observed 8 h after treatment with compound **8v,** and IL-6 levels were still downregulated after 48 h Fig. 5**B**.

2.2.4. 1,3,4-Oxadiazole/chalcone hybrids inhibited STAT3 activity

Because 1,3,4-oxadiazole/chalcone derivatives inhibited EGFR, Src, and IL-6, which a upstream activators of STAT3, the effect of the synthesized compounds on STAT3 activation was evaluated. The results presented in Fig. 6 indicate that 1,3,4-oxadiazole/chalcone derivatives **8a-x** inhibited STAT3 activation. Compounds **8a**, **8n**, and **8v** were the most effective at inhibiting STAT3 activity. Compounds **8b**, **8g-8m**, **8p**, **8q**, **8s**, **8 t**, and **8x** exhibited moderate activities, and the remaining compounds showed low or no activities. Our results also confirmed the type of substitution on phenyl rings influenced activity. For effective STAT3 inhibition, the two phenyl ring should be either unsubstituted or one ring should carry *p*-methoxy group while the second ring should contain 3,4,5-trimethoxy groups.

3. Conclusion

A series of novel 1,3,4-oxadiazole/chalcone hybrids was prepared and identified using different spectroscopic techniques. The compounds we generated showed significant anticancer activity, particularly against leukemia. Compounds **8a, 8n,** and **8v** showed the highest cytotoxicity activity against leukemia cell lines K-562 among the compounds tested. The IC_{50} for the compounds were in the range of 1.95–10.25 μM, compared to cisplatin that has an IC_{50} of 3.21 μM. *In vitro* (one dose) anticancer and MTT assays indicated that compound **8v** exhibited the highest activities against human cancer cells. Compounds, **8a**, **8n** and **8v** displayed the most potent or effective inhibitory activity against EGFR (IC_{50} = 0.24–2.35 μM), Src (IC_{50} = 0.96–6.24 μM), and IL-6 (% of control = 20–23%). Compounds **8a**, **8n**, and **8v** are also the most effective at inhibiting STAT3. It is possible that inhibition of EGFR, Src, and IL-6 by 1,3,4-oxadiazole/chalcone hybrids play roles in the inhibition of STAT3. The inhibition of STAT3 support the potential

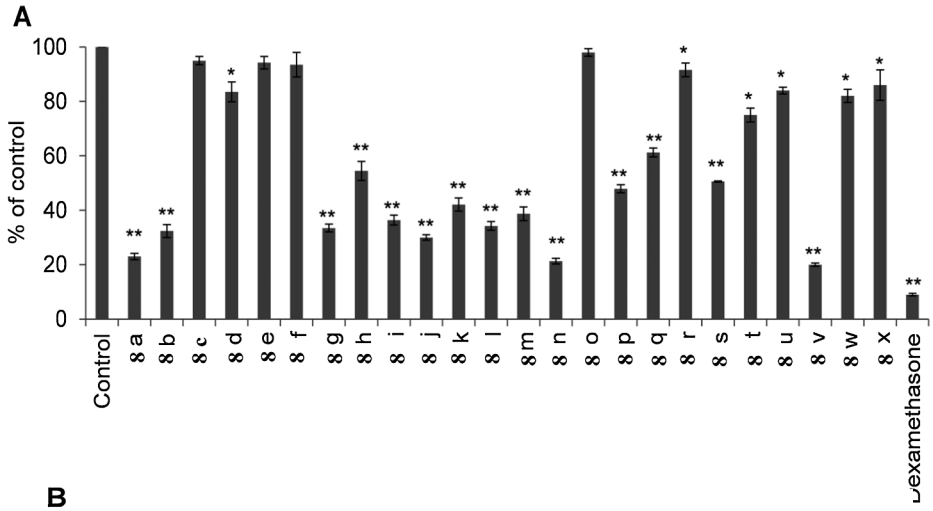

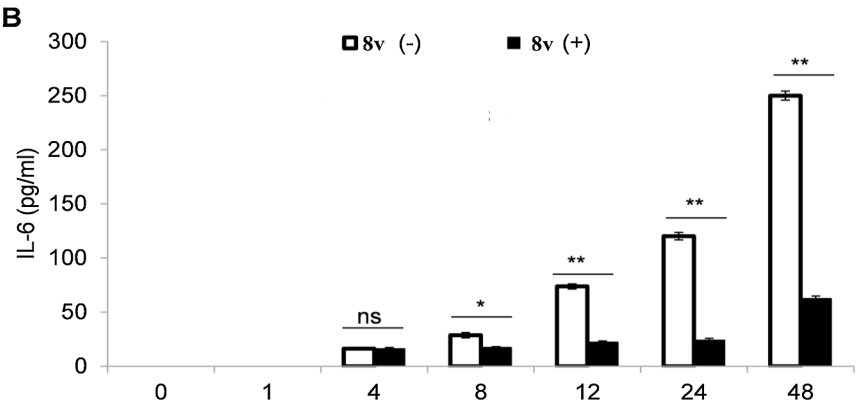

Fig. 5. (A) IL-6 protein expression in K-562 cells 24 h after treatment with 10 μM oxadiazole/chalcone derivatives (**8a-x**) or dexamethasone relative to vehicle treated cells **(B)** Time course effect of **8v** on IL-6 protein expression in K-562 cells treated with 10 μM oxadiazole/chalcone derivative **8v**. The values are expressed as the mean ± SD based on three different experiments. *, $P < 0.05$ and **, $P < 0.005$ indicate a significant difference compared to vehicle treated cells.

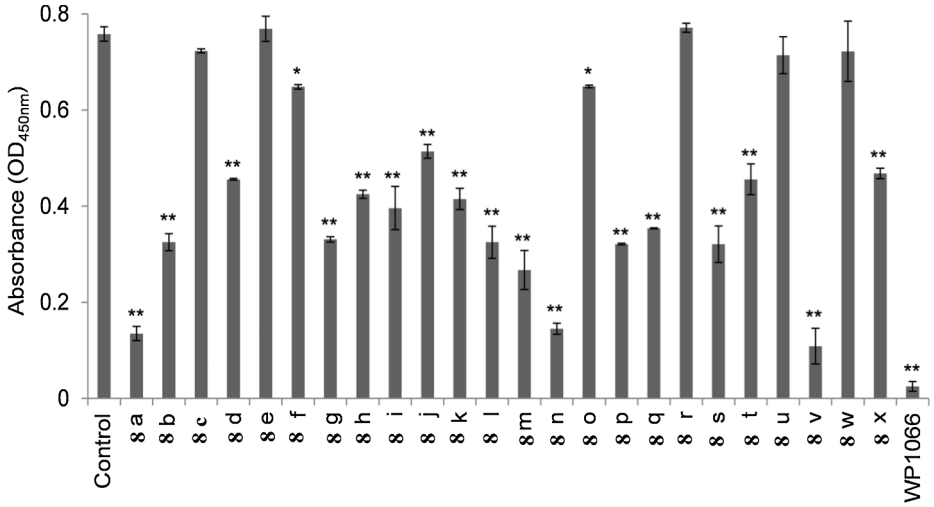

Fig. 6. STAT3 activation assay in K-562 cells treated with 10 μM oxadiazole/chalcone derivatives (**8a-x**), WP1066, or vehicle for 24 h. The values are expressed as the mean ± SD based on three different experiments. *, $P < 0.05$ and **, $P < 0.005$ indicate a significant difference relative to vehicle treated cells.

of 1,3,4-oxadiazole/chalcone hybrids in the treatment of leukemia and prevention of the development of resistance in leukemia cells. However, further studies using *in vivo* models are needed to verify the potential of 1,3,4-oxadiazole/chalcone hybrids as anticancer agents.

4. Experimental section

4.1. Chemistry section

- Analytical grade chemicals and solvents were used. The progress of the reactions was monitored by thin layer chromatography pre-coated Merck silica gel 60 F254 aluminum sheets.
- Melting points were determined on Stuart electro-thermal melting point apparatus in degree Celsius and were uncorrected.
- ^{1}H spectra were recorded on Burker AG, Switzerland, 500 MHz, Faculty of Pharmaceutical Sciences, Umm Al-Qura University, Mecca, Saudi Arabia; chemical shift (δ) were expressed in ppm relative to TMS ($\delta = 0$ PPM) as internal standard and $CDCl_3$ or DMSO-d_6 as a solvent. Chemical shifts (δ) were expressed in parts per million (ppm) and coupling constants (*J*) were expressed in Hertz. The signals were designated as follows: s, singlet; d, doublet; t, triplet; m, multiplet.

- ^{13}C spectra were recorded on Burker AG, Switzerland and 125 MHz, faculty of Pharmaceutical Sciences, Umm Al-Qura University, Mecca, Saudi Arabia using TMS as the reference standard and $CDCl_3$ or DMSO-d_6 as a solvent. Chemical shifts (δ) were expressed in parts per million (ppm).
- LC/MS/MS were carried out using Agilent UPLC/MS/MS 1260 infinity II with 6420 Triple quad LC/MS detector at Faculty of Pharmacy, Minia University, Minia, Egypt
- The purity of the compounds was checked by HPLC.
- Elemental analyses were recorded on Shimadzu GC/ MS-QP5050A, The Regional center for Mycology and Biotechnology, Al-Azhar University, Egypt.

4.1.1. General procedure for the synthesis of substituted ethylbenzoate 2a-e [60]

A mixture of the appropriate substituted benzoic acid **1a-e** (10 mmol), absolute ethanol (20 mL), and concentrated sulfuric acid (2 mL) was heated under reflux for 12–18 h. Excess solvent was removed under reduced pressure. The residue was extracted with ether (2 X 50 mL) and washed with saturated $NaHCO_3$ (2 X 20 mL). The ether layer was dried over anhydrous magnesium sulfate, and ether was evaporated under vacuum to produce the ethyl ester derivatives **2a-e**.

4.1.2. General procedure for the synthesis of substituted benzohydrazides 3a-e [61,62]

Hydrazine hydrate (97%, 30 mmol, 1.5 mL) was added to a solution of the isolated esters **2a–e** (10 mmol) in ethanol (20 mL), and the mixture was heated at reflux for 5–8 h. After cooling, the resulting precipitate was filtered off, washed with water, dried, and crystallized from ethanol.

Benzohydrazide (3a) [62].

White solid (77.2% yield); mp 110–112 °C (Reported mp = 112–114 °C).

4-Chloro-benzohydrazide (3b) [63].

White solid (79.3% yield); mp 195–197 °C (Reported mp = 189–191 °C).

4-Methoxybenohydrazide (3c) [62].

White solid (80.2% yield); mp 134–137 °C (Reported mp = 136–140 °C)

3,4-Dimethoxybenzohydrazide (3d) [62].

White solid (72.7% yield); mp 145–146 °C as reported.

3,4,5-Trimethoxybenzohydrazide (3e) [62].

White solid (72.9% yield); mp 158–160 °C as reported.

4.1.3. General procedure for the synthesis of 5-aryl–1,3,4-oxadiazole-2(3H)-thione derivatives (4a-e) [43,64]

A mixture of the benzohydrazides **3a-e** (0.05 mol), potassium hydroxide (0.05 mol, 2.81 g) and carbon disulfide (0.17 mol, 12.94 g) in 50 mL of absolute ethanol was heated at reflux with stirring for 12 h. The solvent was evaporated under vacuum. The resulting solid was dissolved in water and acidified with 10% HCl. The resulting precipitate was filtered off, washed with water, dried, and recrystallized from ethanol to generate the corresponding oxadiazole derivatives **4a-e** [64].

5-Phenyl-1,3,4-oxadiazole-2(3*H*)-thione (4a) [65].

White solid (76% yield); mp 215–216 °C (Reported mp = 218–220 °C).

5-(4-Chlorophenyl) -1,3,4-oxadiazole-2(3*H*)-thione (4b) [65].

Yellowish white solid (87% yield); mp 172–173 °C (Reported mp = 176–178 °C).

5-(4-Methoxyphenyl)-1,3,4-oxadiazole-2(3*H*)-thione (4c) [65].

White solid (78% yield); mp 192–194 °C (Reported mp = 198–200 °C).

5-(3,4-Dimethoxyphenyl)-1,3,4-oxadiazole-2(3*H*)-thione (4d) [66].

Yellowish white solid (60% yield); mp 238–239 °C (Reported mp = 237–238 °C).

5-(3,4,5-Trimethoxyphenyl)-1,3,4-oxadiazole-2(3*H*)-thione (4e) [67].

Yellowish white solid (79% yield); mp 192–193 °C (Reported mp = 186–188 °C).

4.1.4. General procedure for the synthesis of 1-(4-aminophenyl)-3-arylprop-2-en-1-one (6a-d) [68]

An equimolar amount of *p*-aminoacetophenone (0.1 mol, 13.51 g) and the appropriate aldehyde **5a-d** (0.1 mol), were dissolved in a minimum amount of ethanol, and aqueous NaOH (0.25 mol, 60%) was then added dropwise. The reaction mixture was stirred in ice bath for 30 min then at rt, until the precipitate was formed within 3 h. The precipitate was filtered off and washed thoroughly with cold distilled water and cold methanol (2 × 20 mL). The product was recrystallized from absolute ethanol. The structure of the product was confirmed by mp.

1-(4-Aminophenyl)-3-phenyl prop-2-en-1-one (6a) [59]

Buff solid (77.8% yield); mp 156–157 °C (Reported mp = 157–158 °C).

1-(4-Aminophenyl)-3-(4-chlorophenyl)prop-2-en-1-one (6b) [68].

Yellow solid (80.3% yield); mp 159–160 °C (Reported mp = 158–159 °C).

1-(4-Aminophenyl)-3-(4-methoxyphenyl)prop-2-en-1-one (6c) [68].

Yellow solid (67.3% yield); mp 115–116 °C (Reported mp = 114–115 °C).

1-(4-Aminophenyl)-3-(3,4-dimethoxyphenyl)prop-2-en-1-one (6d) [68].

Yellow solid (82.9% yield); mp 159–160 °C (Reported mp = 158–160 °C).

1-(4-Aminophenyl)-3-(3,4,5-trimethoxyphenyl)prop-2-en-1-one (6e) [68].

Yellow solid (70.4% yield); mp 166–168 °C as reported.

4.1.5. General procedure for the synthesis of 2-bromo-N-(4-(3-arylacryloyl)phenyl)acetamides (7a-e) [59]

To a mixture of the appropriate chalcone **6a-e** (6.30 mmol) in dichloromethane (20 mL) and potassium carbonate (1.302 mmol, 0.18 g) in 100 mL water in an ice bath, bromoacetyl bromide (9.20 mmol, 1.856 g) in 30 mL dichloromethane was added in a dropwise manner with stirring over 30 min. Stirring was continued for 2 h at 0 °C and at rt overnight. The reaction mixture was extracted with dichloromethane (2 × 60 mL) and the organic layer was washed with distilled water (2 × 40 mL), dried over anhydrous sodium sulfate, filtered, evaporated under vacuum and the residue was recrystallized from ethanol.

2-Bromo-*N*-(4-((*E*)-3-phenylacryloyl)phenyl)acetamide (7a) [59].

Pale yellow powder (70.0% yield); mp 157–159 °C (Reported mp = 157–158 °C).

2-Bromo-*N*-(4-(*E*)-3-(4-chlorophenyl)acryloyl)phenyl)acetamide (7b) [68].

Pale yellow powder (71.5% yield); mp 191–192 °C (Reported mp = 190–192 °C).

2-Bromo-*N*-(4-((*E*)-3-(4-methoxyphenyl)acryloyl)phenyl)acetamide (7c) [59].

Pale orange crystal (69.70% yield); mp 155–156 °C (Reported mp = 160–162 °C).

2-Bromo-*N*-(4-((*E*)-3-(3,4-dimethoxyphenyl)acryloyl)phenyl) acetamide (7d) [59].

Yellow powder (71.0% yield); mp 150–151 °C (Reported mp = 149–150 °C).

2-Bromo-*N*-(4-((*E*)-3-(3,4,5-trimethoxyphenyl)acryloyl)phenyl) acetamide (7e) [59].

Yellow powder (78.0% yield); mp 166–167 °C (Reported mp = 160–162 °C).

4.1.6. General procedure for the synthesis of 2-(5-phenyl-1,3,4-oxadiazole-2-ylthio)-N-(4-((E)-3-phenylacryloyl)phenyl)acetamide derivatives (8a-x)

TEA (0.18 mmol, 0.018 g) was added as a base to an equimolar mixture of **4a-e** (0.09 mmol) and compound **7a-e** (0.09 mmol) in acetonitrile. The reaction mixture was stirred at room temperature until the precipitate formed. The resulting precipitate was filtrated off, and the precipitate was then crystallized with acetonitrile to afford the target compounds [59].

4.1.6.1. N-(4-(3-Phenyl)acryloyl)phenyl-2-((5-phenyl-1,3,4-oxadiazol-2-yl)thio)-acetamide (8a).. White solid (0.39 g, 89.0% yield); mp 199–201 °C; ^{1}H NMR (500 MHz, DMSO-d_6) -δ (ppm): 10.89 (s, 1H, NH), 8.18 (d, 2H, *J* = 8.0 Hz, Ar-H), 7.96–7.93 (m, 3H, 2 Ar-H and C<u>H</u>=CH), 7.88–7.87 (m, 2H, Ar-H), 7.80 (d, 2H, *J* = 8.0 Hz, Ar-H), 7.73 (d, 1H, *J* = 16.0 Hz, CH=C<u>H</u>), 7.61 (d, 2H, *J* = 6.0 Hz Ar-H), 7.58 (d, 2H, *J* = 6.0 Hz, Ar-H), 7.49–7.46 (m, 2H, Ar-H), 4.42 (s, 2H, CH_2); ^{13}C NMR (125 MHz, DMSO-d_6) δ (ppm): 188.05, 166.14, 165.66, 163.80, 143.99, 143.50, 135.21, 133.16, 132.54, 131.02, 130.50, 129.90, 129.39, 129.31, 126.84, 123.41, 122.40, 119.07, 37.37; LC−MS *m/z* 440.00 $[M-H]^-$; Anal. Calcd for $C_{25}H_{19}N_3O_3S$: C, 68.01; H, 4.34; N, 9.52; S, 7.26. Found: C, 68.17; H, 4.52; N, 9.80; S, 7.35.

4.1.6.2. N-(4-(3-(4-Chlorophenyl)acryloyl)phenyl)-2-((5-phenyl-1,3,4-oxadiazol-2-yl)thio)acetamide (8b).. Yellow solid (0.29 g, 63.0% yield); mp 250–252 °C; ^{1}H NMR (500 MHz, DMSO-d_6) δ (ppm): 10.85 (s, 1H, NH), 8.20 (d, 2H, *J* = 6.6 Hz, Ar-H), 8.00–7.97 (m, 2H, Ar-H), 7.96–7.93 (m, 3H, 2 Ar-H and CH=C<u>H</u>), 7.79 (d, 2H, *J* = 6.8 Hz, Ar-H), 7.72 (d, 1H, *J* = 15.5 Hz, C<u>H</u>=CH), 7.62–7.58 (m, 3H, Ar-H), 7.54 (d, 2H, *J* = 6.6 Hz, Ar-H), 4.42 (s, 2H, CH_2); ^{13}C NMR (125 MHz, DMSO-d_6) δ (ppm): 187.92, 166.13, 165.67, 163.81, 143.56, 142.51, 135.47, 134.23, 133.07, 132.55, 131.02, 130.56, 129.91, 129.43, 126.85, 123.42, 123.16, 119.07, 37.39; LC−MS *m/z* 475.10 $[M]^+$; Anal. Calcd for $C_{25}H_{18}ClN_3O_3S$: C, 63.09; H, 3.81; N, 8.83; S, 6.74. Found: C, 63.23; H, 3.97; N, 9.06; S, 6.88.

4.1.6.3. N-(4-(3-(3,4-Dimethoxyphenyl)acryloyl)phenyl)-2-((5-phenyl-1,3,4-oxadiazol-2-yl)thio)acetamide (8c).. Yellow solid (0.25 g, 51.0% yield) mp 230–231 °C; ^{1}H NMR (500 MHz, DMSO-d_6) δ (ppm): 10.84 (s, 1H, NH), 8.19 (d, 2H, *J* = 6.4 Hz, Ar-H), 7.97–7.96 (m, 2H, Ar-H), 7.84 (d, 1H, *J* = 15.2 Hz, CH=C<u>H</u>), 7.80 (d, 2H, *J* = 6.4 Hz, Ar-H), 7.70 (d, 1H, *J* = 15.2 Hz, C<u>H</u>=CH), 7.63–7.57 (m, 3H, Ar-H), 7.55 (s, 1H, Ar-H), 7.39 (d, 1H, *J* = 6.0 Hz, Ar-H), 7.03 (d, 1H *J* = 6.0 Hz Ar-H), 4.42 (s, 2H, CH_2), 3.87 (s, 3H, OCH_3), 3.83 (s, 3H, OCH_3); ^{13}C NMR (125 MHz, DMSO-d_6) δ (ppm): 187.89, 166.08, 165.67, 163.82, 151.69, 149.49, 144.53, 143.29, 133.47, 132.55, 130.38, 129.91, 128.05, 126.85, 124.41, 123.42, 119.90, 119.02, 112.01, 111.12, 56.22, 56.07, 37.40; LC−MS *m/z* 501.90 $[M+H]^+$; Anal. Calcd for $C_{27}H_{23}N_3O_5S$: C, 64.66; H, 4.62; N, 8.38; S, 6.39. Found: C, 64.39; H, 4.80; N, 8.54; S, 6.52.

4.1.6.4. N-(4-(3-(3.4.5-Trimethoxyphenyl)acryloyl)phenyl)-2-((5-phenyl-1,3,4-oxadiazol-2-yl)thio)acetamide (8d).. Yellow crystals (0.30 g, 58.0% yield) mp 261–262 °C; ^{1}H NMR (500 MHz, DMSO-d_6) δ (ppm): 10.90 (s, 1H, NH), 8.20 (d, 2H, *J* = 7.5 Hz, Ar-H), 7.97 (d, 2H, *J* = 5.2 Hz, Ar-H), 7.91 (d, 1H, *J* = 15.5 Hz, C<u>H</u>=CH), 7.81 (d, 2H, *J* = 7.5 Hz, Ar-H), 7.69 (d, 1H, *J* = 15.5 Hz, CH=C<u>H</u>), 7.65–7.58 (m, 3H Ar-H), 7.23 (s, 2H, Ar-H), 4.43 (s, 2H, CH_2), 3.87 (s, 6H, $2OCH_3$), 3.72 (s, 3H, OCH_3); ^{13}C NMR (125 MHz, DMSO-d_6) δ (ppm): 187.98, 166.13, 165.68, 163.82, 153.57, 144.53, 143.44, 140.11, 133.26,132.57, 130.77, 130.49, 129.92, 126.84, 123.39, 121.52, 119.04, 106.93, 60.62, 56.60, 37.36; LC−MS *m/z* 529.90 $[M-H]^-$; Anal. Calcd for $C_{28}H_{25}N_3O_6S$: C, 63.26; H, 4.74; N, 7.90; S, 6.03. Found: C, 63.50; H, 4.87; N, 8.21; S, 6.11.

4.1.6.5. 2-((5-(4-Chlorophenyl)-1,3,4-oxadiazol-2-yl)thio)-N-(4-cinnamoyl phenyl)acetamide (8e).. Yellow solid (0.30 g, 63.3% yield) mp 230–231 °C; ^{1}H NMR (500 MHz, DMSO-d_6) δ (ppm): 10.90 (s, 1H, NH), 8.19 (d, 2H, *J* = 7.0 Hz, Ar-H), 7.99–7.97 (m, 2H, Ar-H), 7.93–7.90 (m, 3H, 2 Ar-H and C<u>H</u>=CH), 7.80 (d, 2H, *J* = 7.0 Hz, Ar-H), 7.74 (d, 1H, *J* = 15.5 Hz, CH=C<u>H</u>), 7.66 (d, 2H, *J* = 6.5 Hz, Ar-H), 7.49–7.44 (m, 3H, Ar-H), 4.43 (s, 2H, CH_2); ^{13}CNMR (125 MHz, DMSO-d_6) δ (ppm): 188.05, 166.08, 164.92, 164.11, 143.99, 143.49, 137.24, 135.23, 133.17, 131.02, 130.50, 130.09, 129.39, 129.31, 128.66, 122.41, 122.32, 119.08, 37.38; LC−MS *m/z* 474.10 $[M-H]^-$; Anal. Calcd for $C_{25}H_{18}ClN_3O_3S$: C, 63.09; H, 3.81; N, 8.83; S, 6.74. Found: C, 63.28; H, 3.75; N, 8.97; S, 6.82.

4.1.6.6. 2-((5-(4-Chlorophenyl)-1,3,4-oxadiazol-2-yl)thio)-N-(4-(3-(4-chloro-phenyl)acryloyl)phenyl)acetamide (8f).. Yellow solid (0.39 g, 77.0% yield) mp 181–182 °C; ^{1}H NMR (500 MHz, DMSO-d_6) δ (ppm): 10.86 (s, 1H, NH), 8.18 (d, 2H, *J* = 8.0 Hz, Ar-H), 7.98–7.97 (m, 3H, 2 Ar-H and CH=C<u>H</u>), 7.93 (d, 2H, *J* = 8.0 Hz, Ar-H), 7.78 (d, 2H, *J* = 8.0 Hz, Ar-H), 7.71 (d, 1H, *J* = 15.0 Hz, CH=C<u>H</u>), 7.66 (d, 2H, *J* = 7.5 Hz, Ar-H), 7.53 (d, 2H *J* = 8.0 Hz, Ar-H), 4.42 (s, 2H, CH_2); ^{13}C NMR (125 MHz, DMSO-d_6) δ (ppm): 187.93, 166.09, 164.92, 164.11, 137.25, 135.47, 134.21, 133.06, 131.02, 130.56, 130.09, 129.47, 129.43, 129.01, 128.66, 123.14, 122.31, 119.06, 37.38; LC−MS *m/z* 509.90 $[M+H]^+$; Anal. Calcd for $C_{25}H_{17}Cl_2N_3O_3S$: C, 58.83; H, 3.36; N, 8.23; S, 6.28. Found: C, 59.17; H, 3.42; N, 8.04; S, 6.12.

4.1.6.7. 2-(5-(4-Chlorophenyl)-1,3,4-oxadiazol-2-ylthio)-N-(4-(3-(4-methoxy- phenyl)acryloyl)phenyl)acetamide (8g).. Yellow crystals (0.31 g, 62.0% yield) mp 227–228 °C; ^{1}H NMR (500 MHz DMSO-d_6) δ (ppm): 10.83 (s, 1H, NH), 8.17 (d, 2H, *J* = 6.0 Hz, Ar-H), 7.98 (d, 2H, *J* = 5.7 Hz, Ar-H), 7.86 (d, 2H, *J* = 5.7 Hz, Ar-H), 7.79–7.77 (m, 3H, 2 Ar-H + CH=C<u>H</u>), 7.71 (d, 1H, *J* = 15.00 Hz, C<u>H</u>=CH), 7.67 (d, 2H, *J* = 6.0 Hz, Ar-H), 7.03 (d, 2H, *J* = 5.9 Hz, Ar-H), 4.43 (s, 2H, CH_2), 3.83 (s, 3H, OCH_3); ^{13}C NMR (125 MHz, DMSO-d_6) δ (ppm): 188.83, 166.02, 164.92, 164.12, 161.98, 161.77, 144.95, 143.98, 143.26, 139.02, 131.41, 131.19, 130.33, 130.08, 128.64, 122.31, 119.03, 114.87, 55.84, 37.37; LC−MS *m/z* 504.00 $[M-H]^-$; Anal. Calcd for $C_{26}H_{20}ClN_3O_4S$: C, 61.72; H, 3.98; N, 8.30; S, 6.34. Found: C, 61.95; H, 4.12; N, 8.59; S, 6.51.

4.1.6.8. 2-(5-(4-Chlorophenyl)-1,3,4-oxadiazol-2-ylthio)-N-(4-(3-(3,4-dimethoxy- phenyl)acryloyl)phenyl)acetamide (8h).. Yellow solid (0.38 g, 71.4% yield) mp 215–216 °C; ^{1}H NMR (500 MHz, $CDCl_3$) δ (ppm): 10.88 (s, 1H, NH), 8.19 (d, 2H, *J* = 6.6 Hz, Ar-H), 7.98 (d, 2H, *J* = 6.1 Hz, Ar-H), 7.84 (d, 1H, *J* = 15.3 Hz, C<u>H</u>=CH), 7.79 (d, 2H, *J* = 6.6 Hz, Ar-H), 7.71–7.66 (m, 3H, 2 Ar-H + CH=C<u>H</u>), 7.55 (s, 1H, Ar-H), 7.39 (d, 1H, *J* = 6.1 Hz, Ar-H), 7.03 (d, 1H, *J* = 6.1 Hz, Ar-H), 4.43 (s, 2H, CH_2), 3.87 (s, 3H, OCH_3), 3.83 (s, 3H, OCH_3); ^{13}CNMR (125 MHz, $CDCl_3$) δ (ppm): 187.90, 166.02, 164.93, 164.13, 151.69, 149.49, 144.53, 143.27, 137.25, 133.47, 130.38, 130.09, 128.66, 128.05, 124.41, 122.32, 119.90, 119.02, 112.02, 111.12, 56.22, 56.07, 37.40; LC−MS *m/z* 534.00 $[M-H]^-$; Anal. Calcd for $C_{27}H_{22}ClN_3O_5S$: C, 60.50; H, 4.14; N, 7.84; S, 5.98. Found: C, 60.38; H, 4.27; N, 8.11; S, 6.15.

4.1.6.9. 2-(5-(4-Chlorophenyl)-1,3,4-oxadiazol-2-ylthio)-N-(4-(3-(3,4,5-trimethoxyphenyl)acryloyl)phenyl)acetamide (8i).. Yellow crystals (0.40 g, 71.0% yield) mp 261–262 °C; ^{1}H NMR (500 MHz, DMSO-d_6 δ (ppm): 10.85 (s, 1H, NH), 8.20 (d, 2H, *J* = 7.1 Hz, Ar-H), 7.98 (d, 2H, *J* = 6.9 Hz, Ar-H), 7.91 (d, 1H, *J* = 15.4, C<u>H</u>=CH), 7.80 (d, 2H, *J* = 7.1 Hz, Ar-H), 7.71–7.67 (m, 3H, 2 Ar-H + CH=C<u>H</u>), 7.24 (s, 2H, Ar-H), 4.43 (s, 2H, CH_2), 3.87 (s, 6H, $2OCH_3$), 3.72 (s, 3H, OCH_3); ^{13}C NMR (125 MHz, DMSO-d_6) δ (ppm): 187.96, 166.05, 164.93, 164.13, 153.58, 144.52, 143.41, 140.05, 137.25, 133.29, 130.78, 130.49,

130.10, 128.66, 122.32, 121.53, 119.03, 106.96, 60.62, 57.30, 56.61, 37.41; Anal. Calcd for $C_{28}H_{24}ClN_3O_6S$: C, 59.41; H, 4.27; N, 7.42; S, 5.67. Found: C, 59.58; H, 4.35; N, 7.60; S, 5.74.

4.1.6.10. 2-(5-(4-Methoxyphenyl)-1,3,4-oxadiazol-2-ylthio)-N-(4-(3-phenyl acryloyl)phenyl)acetamide (8j).. Yellow solid (0.39 g, 84.0% yield) mp 195–197 °C; ^{1}H NMR (500 MHz, $CDCl_3$) δ (ppm): 9.90 (s, 1H, NH), 8.03 (d, 2H, *J* = 7.0 Hz, Ar-H), 7.96 (d, 2H, *J* = 7.0 Hz, Ar-H), 7.81 (d, 1H, *J* = 15.0 Hz, CH═CH), 7.77–7.75 (m, 1H, Ar-H), 7.66 (d, 2H, *J* = 6.0 Hz, Ar-H), 7.53 (d, 1H, *J* = 15.0, CH═CH), 7.45–7.42 (m, 4H, Ar-H), 7.02 (d, 2H, *J* = 6.0 Hz, Ar-H), 4.11 (s, 2H, CH_2), 3.90 (s, 3H, OCH_3); ^{13}C NMR (125 MHz, $CDCl_3$) δ (ppm): 189.01, 166.56, 165.84, 164.44, 162.84, 144.59, 141.96, 130.49, 129.92, 128.97, 128.75, 128.47, 121.83, 119.36, 115.17, 114.83, 114.73, 114.12, 55.56, 36.50; Anal. Calcd for $C_{26}H_{21}N_3O_4S$: C, 66.23; H, 4.49; N, 8.91; S, 6.80. Found: C, 66.06; H, 4.62; N, 9.18; S, 6.59.

4.1.6.11. 2-(5-(4-Methoxyphenyl)-1,3,4-oxadiazol-2-ylthio)-N-(4-(3-(4-chloro- phenyl)acryloyl)phenyl)acetamide (8k).. Yellow solid (0.37 g, 75.0% yield) mp 250–251 °C; ^{1}H NMR (500 MHz, DMSO-d_6) δ (ppm): 10.83 (s, 1H, NH), 8.19 (d, 2H, *J* = 6.3 Hz, Ar-H), 7.98 (d, 1H, *J* = 16.0 Hz, CH═CH), 7.94 (d, 2H, *J* = 5.7 Hz, Ar-H), 7.89 (d, 2H, *J* = 6.2 Hz, Ar-H), 7.79 (d, 2H, *J* = 6.2 Hz, Ar-H), 7.72 (d, 1H, *J* = 16.0 Hz, CH═CH), 7.54 (d, 2H, *J* = 5.7 Hz, Ar-H), 7.12 (d, 2H, *J* = 6.3 Hz, Ar-H), 4.39 (s, 2H, CH_2), 3.84 (s, 3H, OCH_3); ^{13}C NMR (125 MHz, DMSO-d_6) δ (ppm): 188.04, 166.11, 165.61, 163.62, 153.92, 144.01, 143.48, 141.02, 135.21, 133.17, 131.03, 130.50, 129.40, 129.31, 122.38, 119.06, 118.59, 104.23, 56.59, 37.41; LC−MS *m/z* 504.00 $[M-H]^-$; Anal. Calcd for $C_{26}H_{20}ClN_3O_4S$: C, 61.72; H, 3.98; N, 8.30; S, 6.34. Found: C, 61.97; H, 4.11; N, 8.54; S, 6.47.

4.1.6.12. 2-(5-(4-Methoxyphenyl)-1,3,4-oxadiazol-2-ylthio)-N-(4-((E)-3-(4-methoxyphenyl)acryloyl)phenyl)acetamide (8l).. Yellow solid (0.37 g, 75.0% yield) mp 183–185 °C; ^{1}H NMR (500 MHz, DMSO-d_6) δ (ppm): 10.86 (s, 1H, NH), 8.12 (d, 2H, *J* = 8.0 Hz, Ar-H), 7.86 (d, 2H, *J* = 7.5 Hz, Ar-H), 7.81 (d, 2H, *J* = 8.0 Hz, Ar-H), 7.75–7.71 (m, 3H, Ar-H and CH═CH), 7.68 (d, 1H, *J* = 15.0 *Hz*, CH═CH) 7.08 (d, 2H, *J* = 8.0 *Hz,* Ar-H), 7.00 (d, 2H, *J* = 7.5 Hz*,* Ar-H), 4.32 (s, 2H, CH_2), 3.82 (s, 3H, OCH_3), 3.80 (s, 3H, OCH_3); ^{13}C NMR (125 MHz, DMSO-d_6) δ (ppm): 187.91, 166.15, 165.63, 162.94, 162.53, 161.77, 143.90, 143.32, 133.43, 131.20, 130.33, 128.72, 127.81, 119.85, 119.03, 115.74, 115.33, 114.87, 56.12, 55.99, 37.24; LC−MS *m/z* 500.10 $[M-H]^-$; Anal. Calcd for $C_{27}H_{23}N_3O_5S$: C, 64.66; H, 4.62; N, 8.38; S, 6.39. Found: C, 64.49; H, 4.80; N, 8.57; S, 6.21.

4.1.6.13. 2-(5-(4-Methoxyphenyl)-1,3,4-oxadiazol-2-ylthio)-N-(4–3-(3,4-dimethoxyphenyl)acryloyl)phenyl)acetamide (8m).. Yellow crystals (0.40 g, 76.9% yield) mp 193–195 °C; ^{1}H NMR (500 MHz, DMSO-d_6) δ (ppm): 10.83 (s, 1H, NH), 8.19 (d, 2H, *J* = 7.3 Hz, Ar-H), 7.90 (d, 2H, *J* = 7.6 Hz, Ar-H), 7.84 (d, 1H, *J* = 15.2 Hz, CH═CH), 7.79 (d, 2H, *J* = 7.3 Hz, Ar-H), 7.70 (d, 1H, *J* = 15.2 Hz, CH═CH), 7.55 (s, 1H, Ar-H), 7.39 (d, 1H, *J* = 7.1 Hz, Ar-H), 7.12 (d, 2H, *J* = 7.6 Hz, Ar-H), 7.03 (d, 1H, *J* = 7.1 Hz, Ar-H), 4.39 (s, 2H, CH_2), 3.87 (s, 3H, OCH_3), 3.85 (s, 3H, OCH_3), 3.83 (s, 3H, OCH_3); ^{13}C NMR (125 MHz, DMSO-d_6) δ (ppm): 187.90, 166.13, 165.64, 162.95, 162.55, 151.70, 149.49, 144.53, 143.30, 133.46, 130.38, 128.73, 128.05, 124.41, 119.90, 119.02, 115.75, 115.36, 112.02, 111.13, 56.22, 56.08, 56.01, 37.38; Anal. Calcd for $C_{28}H_{25}N_3O_6S$: C, 63.26; H, 4.74; N, 7.90; S, 6.03. Found: C, 63.58; H, 4.89; N, 7.81; S, 6.22.

4.1.6.14. 2-(5-(4-Methoxyphenyl)-1,3,4-oxadiazol-2-ylthio)-N-(4-(3-(3,4,5-tri-methoxyphenyl)acryloyl)phenyl)acetamide (8n).. Yellow solid (0.43 g, 83.3% yield) mp 220–221 °C; ^{1}H NMR (500 MHz, DMSO-d_6) δ (ppm): 10.84 (s, 1H, NH), 8.20 (d, 2H, *J* = 5.7 Hz, Ar-H), 7.91–7.89 (m, 3H, 2 Ar-H and CH═CH), 7.80 (d, 2H, *J* = 5.5 Hz, Ar-H), 7.69 (d, 1H, *J* = 15.3 Hz, CH═CH), 7.24 (s, 2H, Ar-H), 7.12 (d, 2H, *J* = 5.7 Hz, Ar-H), 4.40 (s, 2H, CH_2), 3.87 (s, 6H, 2 OCH_3), 3.85 (s, 3H, OCH_3), 3.72 (s, 3H, OCH_3); ^{13}C NMR (125 MHz, DMSO-d_6) δ (ppm): 187.95, 166.17, 165.63, 162.96, 162.54, 153.58, 144.53, 143.46, 140.10, 133.26, 130.78, 130.50, 128.72, 121.51, 119.01, 115.74, 115.35, 106.93, 56.59, 55.99, 53.91, 37.37; LC−MS *m/z* 560.10 $[M-H]^-$; Anal. Calcd for $C_{29}H_{27}N_3O_7S$: C, 62.02; H, 4.85; N, 7.48; S, 5.71. Found: C, 61.89; H, 4.97; N, 7.67; S, 5.84.

4.1.6.15. N-(4-Cinnamoylphenyl)-2-((5-(3,4-dimethoxyphenyl)-1,3,4-oxadiazol-2-yl)thio)acetamide (8o).. Yellow powder (0.41 g, 83.3% yield) mp 200–202 °C; ^{1}H NMR (500 MHz, DMSO-d_6) δ (ppm): 11.25 (s, 1H, NH), 8.18 (d, 2H, *J* = 7.3 Hz, Ar-H), 7.96 (d, 1H, *J* = 15.3 Hz, CH═CH), 7.91–7.88 (m, 3H, Ar-H), 7.84 (d, 2H, *J* = 7.3 Hz, Ar-H), 7.73 (d, 1H, *J* = 15.3 Hz, CH═CH), 7.55 (d, 1H, *J* = 7.7 Hz, Ar-H), 7.48–7.45 (m, 3H, Ar-H), 7.13 (d, 1H, *J* = 7.7 Hz, Ar-H), 4.45 (s, 2H, CH_2), 3.84 (s, 3H, OCH_3), 3.82 (s, 3H, OCH_3); ^{13}C NMR (125 MHz, DMSO-d_6) δ (ppm): 188.05, 166.19, 165.72, 163.00, 152.34, 149.54, 143.99, 143.54, 135.21, 131.02, 130.48, 129.39, 129.31, 122.39, 120.45, 119.60, 119.06, 115.65, 112.46, 109.45, 56.49, 56.18, 37.36; LC−MS *m/z* 500.10 $[M-H]^-$; Anal. Calcd for $C_{27}H_{23}N_3O_5S$: C, 64.66; H, 4.62; N, 8.38; S, 6.39. Found: C, 64.89; H, 4.76; N, 8.62; S, 6.50.

4.1.6.16. N-(4-(3-(4-chlorophenyl)acryloyl)phenyl)-2-((5-(3,4-dimethoxyphenyl)-1,3,4-oxadiazol-2-yl)thio)acetamide (8p).. Pale yellow powder (0.32 g, 60.7% yield) mp 239–241 °C; ^{1}H NMR (500 MHz, DMSO-d_6) δ (ppm): 10.88 (s, 1H, NH), 8.18 (d, 2H, *J* = 8.1 Hz, Ar-H), 7.97 (d, 1H, *J* = 15.6 Hz, CH═CH), 7.93 (d, 2H, *J* = 7.8 Hz, Ar-H), 7.78 (d, 2H, *J* = 8.1 Hz, Ar-H), 7.71 (d, 1H, *J* = 15.6 Hz, CH═CH), 7.53 (d, 3H, *J* = 8.4 Hz, Ar-H), 7.42 (s, 1H, Ar-H), 7.12 (d, 1H, *J* = 8.4 Hz, Ar-H), 4.39 (s, 2H, CH_2), 3.83 (s, 3H, OCH_3), 3.80 (s, 3H, OCH_3); ^{13}C NMR (125 MHz, DMSO-d_6) δ (ppm): 187.94, 166.19, 165.73, 163.01, 152.33, 149.52, 143.57, 142.53, 135.48, 134.19, 131.01, 130.55, 129.60, 129.43, 123.10, 120.45, 119.06, 115.62, 112.44, 109.40, 56.17, 56.08, 37.36; Anal. Calcd for $C_{27}H_{22}ClN_3O_5S$: C, 60.50; H, 4.14; N, 7.84; S, 5.98. Found: C, 60.76; H, 4.23; N, 8.11; S, 6.09.

4.1.6.17. 2-((5-(3,4-Dimethoxyphenyl)-1,3,4-oxadiazol-2-yl)thio)-N-(4-(3-(4-methoxyphenyl)acryloyl)phenyl)acetamide (8q).. Yellow solid (0.34 g, 65.3% yield) mp 189–190 °C; ^{1}H NMR (500 MHz, DMSO-d_6) δ (ppm): 10.82 (s, 1H, NH), 8.17 (d, 2H, *J* = 6.4 Hz, Ar-H), 7.86 (d, 2H, *J* = 6.0 Hz, Ar-H), 7.80–7.77 (m, 3H, 2 Ar-H + CH═CH), 7.71 (d, 1H, *J* = 15.3 Hz, CH═CH), 7.54 (d, 1H, *J* = 6.3 Hz, Ar-H), 7.43 (s, 1H, Ar-H), 7.13 (d, 1H, *J* = 6.3, Ar-H), 7.03 (d, 2H, *J* = 6.4 Hz, Ar-H), 4.40 (s, 2H, CH_2), 3.84 (s, 6H, 2 OCH_3), 3.82 (s, 3H, OCH_3); ^{13}C NMR (125 MHz, DMSO-d_6) δ (ppm): 187.69, 166.23, 165.72, 162.99, 161.76, 152.32, 149.52, 143.97, 143.42, 133.37, 131.21, 130.28, 127.84, 120.47, 119.86, 119.04, 115.64, 114.88, 112.46, 109.46, 56.19, 56.13, 55.86, 37.26; LC−MS *m/z* 530.20 $[M-H]^-$; Anal. Calcd for $C_{28}H_{25}N_3O_6S$: C, 63.26; H, 4.74; N, 7.90; S, 6.03. Found: C, 63.14; H, 4.89; N, 8.16; S, 6.15.

4.1.6.18. 2-((5-(3,4-Dimethoxyphenyl)-1,3,4-oxadiazol-2-yl)thio)-N-(4-(3-(3,4-di- methoxyphenyl)acryloyl)phenyl)acetamide (8r).. Yellow solid (0.37 g, 66.0% yield) mp 213–214 °C; ^{1}H NMR (500 MHz, DMSO-d_6) δ (ppm): 10.83 (s, 1H, NH), 8.19 (d, 2H, *J* = 6.1 Hz, Ar-H), 7.84 (d, 1H, *J* = 15.2 Hz, CH═CH), 7.79 (d, 2H, *J* = 6.1 Hz, Ar-H), 7.70 (d, 1H, *J* = 15.2 Hz, CH═CH), 7.55–7.51 (m, 2H, Ar-H), 7.43 (s, 1H, Ar-H), 7.39 (d, 1H, *J* = 5.8 Hz, Ar-H), 7.13 (d, 1H, *J* = 6.6 Hz, Ar-H), 7.03 (d, 1H, *J* = 5.8, Ar-H), 4.40 (s, 2H, CH_2), 3.87 (s, 3H, OCH_3), 3.84 (s, 3H, OCH_3), 3.82 (s, 6H, 2 OCH_3); ^{13}C NMR (DMSO-d_6) δ (ppm): 187.90, 166.11, 165.73, 163.02, 152.36, 151.69, 149.56, 149.49, 144.53, 143.30, 133.47, 130.37, 128.05, 124.40, 120.45, 119.89, 119.01, 115.66, 112.47, 112.01, 111.12, 109.47, 56.22, 56.19, 56.11, 56.07, 37.42; LC−MS *m/z* 562.00 $[M+H]^+$; Anal. Calcd for $C_{29}H_{27}N_3O_7S$: C, 62.02; H, 4.85; N, 7.48; S, 5.71. Found: C, 62.27; H, 4.97; N, 7.62; S, 5.89.

4.1.6.19. 2-((5-(3,4-Dimethoxyphenyl)-1,3,4-oxadiazol-2-yl)thio)-N-(4-(3-(3,4,5-trimethoxyphenyl)acryloyl)phenyl)acetamide (8s).. Yellow solid (0.42 g, 72.2% yield) mp 210–212 °C; ^{1}H NMR (500 MHz, $CDCl_3$) δ (ppm): 9.86 (s, 1H, NH), 8.02 (d, 2H, *J* = 8.0 Hz, Ar-H), 7.75–7.70 (m, 3H, 2 Ar-H, CH=CH), 7.60 (d, 1H, *J* = 7.0 Hz, Ar-H), 7.53 (s, 1H, Ar-H), 7.40 (d, 1H, *J* = 15.0 Hz, CH=CH), 6.99 (d, 1H, *J* = 8.0, Ar-H), 6.87 (s, 2H, Ar-H), 4.09 (s, 2H, CH_2), 3.98 (s, 6H, 2OCH_3), 3.94 (s, 6H, 2 OCH_3), 3.92 (s, 3H, OCH_3); ^{13}C NMR (125 MHz, $CDCl_3$) δ (ppm): 189.05, 166.62, 165.87, 164.53, 153.48, 152.51, 149.47, 144.83, 141.86, 140.35, 134.15, 130.42, 129.93, 121.19, 120.61, 119.33, 115.26, 111.21, 109.14, 105.60, 61.04, 56.25, 56.21, 56.13, 36.35; LC−MS *m/z* 590.20 $[M-H]^-$; Anal. Calcd for $C_{30}H_{29}N_3O_8S$: C, 60.90; H, 4.94; N, 7.10; S, 5.42. Found: C, 61.23; H, 4.89; N, 7.24; S, 5.58.

4.1.6.20. N-(4-Cinnamoylphenyl)-2-((5-(3,4,5-trimethoxyphenyl)-1,3,4-oxadiazol-2-yl)thio)acetamide (8t).. Pale yellow crystals (0.38 g,71.8% yield) mp 219–221 °C; ^{1}H NMR (500 MHz, DMSO-d_6) δ (ppm): 10.84 (s, 1H, NH), 8.19 (d, 2H, *J* = 6.7 Hz, Ar-H), 7.95 (d, 1H, *J* = 15.5 Hz, CH=CH), 7.90–7.88 (m, 2H, Ar), 7.79 (d, 2H, *J* = 6.7 Hz, Ar-H), 7.74 (d, 1H, *J* = 15.5 Hz, CH=CH), 7.49–7.45 (m, 3H, Ar-H), 7.22 (s, 2H, Ar-H), 4.42 (s, 2H, CH_2), 3.84 (s, 6H, 2OCH_3), 3.74 (s, 3H, OCH_3), ^{13}C NMR (125 MHz, $CDCl_3$) δ (ppm): 188.98, 166.54, 165.74, 164.83, 153.80, 144.64, 141.89, 141.61, 130.52, 129.92, 129.50, 128.97, 128.46, 121.79, 120.06, 119.31, 117.85, 104.11, 61.07, 56.43, 36.39; LC−MS *m/z* 531.10 $[M]^-$; Anal. Calcd for $C_{28}H_{25}N_3O_6S$: C, 63.26; H, 4.74; N, 7.90; S, 6.03. Found: C, 63.54; H, 4.65; N, 8.12; S, 6.15.

4.1.6.21. N-(4-(3-(4-Chlorophenyl)acryloyl)phenyl)-2-((5-(3,4,5-trimethoxy- phenyl)-1,3,4-oxadiazol-2-yl)thio)acetamide (8u).. Yellow solid (0.49 g, 87.5% yield) mp 259–261 °C; ^{1}H NMR (500 MHz, DMSO-d_6) δ (ppm): 10.85 (s, 1H, NH), 8.19 (d, 2H, *J* = 6.6 Hz, Ar-H), 7.98 (d, 1H, *J* = 16.0 Hz, CH=CH), 7.94 (d, 2H, *J* = 6.4 Hz, Ar-H), 7.79 (d, 2H, *J* = 6.4 Hz, Ar-H), 7.72 (d, 1H, *J* = 16.0 Hz, CH=CH), 7.54 (d, 2H, *J* = 6.6 Hz, Ar-H), 7.22 (s, 2H, Ar-H), 4.80 (s, 2H, CH_2), 3.97 (s, 6H, 2 OCH_3), 3.95 (s, 3H, OCH_3), ^{13}C NMR (125 MHz, DMSO-d_6) δ (ppm): 187.91, 166.12, 165.62, 163.62, 153.93, 143.56, 142.52, 141.03, 135.47, 134.22, 133.08, 131.02, 130.55, 129.43, 123.14, 119.05, 118.59, 104.25, 60.71, 56.60, 37.43; LC−MS *m/z* 564.10 $[M-H]^-$; Anal. Calcd for $C_{28}H_{24}ClN_3O_6S$: C, 59.41; H, 4.27; N, 7.42; S, 5.67. Found: C, 59.32; H, 4.35; N, 7.68; S, 5.73.

4.1.6.22. N-(4-(3-(4-Methoxyphenyl)acryloyl)phenyl)-2-((5-(3,4,5-trimethoxy- phenyl)-1,3,4-oxadiazol-2-yl)thio)acetamide (8v).. Yellow crystals (0.47 g, 84.0% yield) mp 211–212 °C; ^{1}H NMR (500 MHz, DMSO-d_6) δ (ppm): 10.83 (s, 1H, NH), 8.17 (d, 2H, *J* = 6.9 Hz, Ar-H), 7.86–7.82 (m, 3H, 2 Ar-H + CH=CH), 7.78 (d, 2H, *J* = 7.6 Hz, Ar-H), 7.71 (d, 1H, *J* = 15.2 Hz, CH=CH), 7.22 (s, 2H, Ar-H), 7.03 (d, 2H, *J* = 6.9, Ar-H), 4.42 (s, 2H, CH_2), 3.84 (s, 9H, 3OCH_3), 3.74 (s, 3H, OCH_3); ^{13}C NMR (125 MHz, DMSO-d_6) δ (ppm): 187.96, 169.22, 165.75, 165.02, 161.78, 153.90, 144.00, 143.22, 140.82, 133.50, 131.21, 130.26, 127.84, 119.84, 119.21, 118.83, 114.88, 104.13, 60.69, 56.62, 55.86, 37.37; LC−MS *m/z* 561.90 $[M+H]^+$; Anal. Calcd for $C_{29}H_{27}N_3O_7S$: C, 62.02; H, 4.85; N, 7.48; S, 5.71. Found: C, 62.19; H, 4.98; N, 7.67; S, 5.92.

4.1.6.23. N-(4-(3-(3,4-Dimethoxyphenyl)acryloyl)phenyl)-2-((5-(3,4,5-trimethoxyphenyl)-1,3,4-oxadiazol-2-yl)thio)acetamide (8w).. Yellow solid (0.32 g, 55.0% yield) mp 168–170 °C; ^{1}H NMR (500 MHz, DMSO-d_6) δ (ppm): 10.98 (s, 1H, NH), 8.17 (d, 2H, *J* = 8.0 Hz, Ar-H), 7.83–7.79 (m, 3H, 2 Ar-H + CH=CH), 7.80 (d, 1H, *J* = 15.0 Hz, CH=CH), 7.53 (s, 1H, Ar-H), 7.38 (d, 1H, *J* = 8.0 Hz Ar-H), 7.21 (s, 2H, Ar-H), 7.01 (d, 1H *J* = 8.0 Hz, Ar- H), 4.43 (s, 2H, CH_2), 3.86 (s, 6H, 2 OCH_3), 3.83 (s, 6H, 2 OCH_3), 3.73 (s, 3H, OCH_3); ^{13}C NMR (125 MHz, DMSO-d_6) δ (ppm): 188.00, 166.12, 165.61, 163.62, 153.92, 151.68, 149.47, 144.53, 143.35, 141.00, 133.43, 130.35, 128.03, 124.41, 119.88, 119.01, 118.59, 112.00, 111.10, 104.23, 60.70, 56.60, 56.21, 56.06, 37.36; Anal. Calcd for $C_{30}H_{29}N_3O_8S$: C, 60.90; H, 4.94; N, 7.10; S, 5.42. Found: C, 61.23; H, 5.12; N, 7.37; S, 5.39.

4.1.6.24. 2-((5-(3,4,5-Trimethoxyphenyl)-1,3,4-oxadiazol-2-yl)thio)-N-(4-(3-(3,4,5-trimethoxyphenyl)acryloyl)phenyl)acetamide (8x).. Yellow solid (0.49 g, 80.0% yield) mp 196–198 °C; ^{1}H NMR (500 MHz, $CDCl_3$) δ (ppm): 9.74 (s, 1H, NH), 8.02 (d, 2H, *J* = 8.1 Hz, Ar-H), 7.74–7.70 (m, 3H, 2 Ar-H + CH=CH), 7.39 (d, 1H, *J* = 15.6 Hz, CH=CH), 7.24 (s, 2H, Ar-H), 6.87 (s, 2H, Ar-H), 4.09 (s, 2H, CH_2), 3.95 (s, 6H, 2 OCH_3), 3.94 (s, 9H, 3 OCH_3), 3.92 (s, 3H, OCH_3), ^{13}C NMR (125 MHz, $CDCl_3$) δ (ppm): 189.03, 166.57, 165.77, 164.79, 153.79, 153.49, 144.84, 141.80, 141.58, 140.44, 134.22, 130.41, 129.91, 121.18, 119.31, 117.87, 105.69, 104.08, 61.07, 61.02, 56.41, 56.25, 36.31; LC−MS *m/z* 620.10 $[M-H]^-$; Anal. Calcd for $C_{31}H_{31}N_3O_9S$: C, 59.89; H, 5.03; N, 6.76; S, 5.16. Found: C, 59.71; H, 5.21; N, 6.94; S, 5.24.

4.2. Biology section

4.2.1. Cell culture and reagents

Human leukemia cell lines (K-562, KG1a, and Jurkat) were obtained from the American Type Culture Collection (ATCC; Manassas, VA, USA) and were cultured in Iscove's Modified Dulbecco's Medium (IMDM, Sigma-Aldrich) or Roswell Park Memorial Institute Medium (RPMI 1640, Sigma-Aldrich), containing 10% fetal bovine serum (FBS; Sigma-Aldrich) in a humidified atmosphere with 5% CO_2 at 37 °C. Cisplatin, dasatinib, dexamethasone, gefitinib, and WP1066 were purchased from Sigma-Aldrich. All chemicals used in this study were analytical or cell-culture grade.

4.2.2. Proliferation assay

The methodology for NCI anticancer screening has been described in detail elsewhere (http://www.dtp.nci.nih.gov). Briefly, the primary anticancer assay was performed at approximately 60 human tumor cell lines panel derived from nine neoplastic diseases, in accordance with the protocol of the Drug Evaluation Branch, National Cancer Institute, Bethesda. Tested compounds were added to the cells at a single concentration (10^{-5} M) and were incubated for 48 h. Endpoint determinations were made with a protein binding dye, SRB. Absorbance was evaluated spectrophotometrically and results for each tested compound were reported as the percent of the growth of the treated cells when compared to untreated cells.

Compound **8v,** which showed significant cell growth inhibition in the One-Dose Screen, was evaluated against the 58 cell panel at five different concentrations by a dissolving the drug in dimethyl sulfoxide. After drug addition, cells were incubated at 37° C, 5% CO_2, 95% air and 100% relative humidity for 48 h, stained by SRB, and the absorbance was evaluated spectrophotometrically by using an automated plate. The growth percentage was calculated at different drug concentrations levels and at different time points.

4.2.3. Anti-proliferative assay [69,70]

Cytotoxicity was measured using the MTT assay. Leukemia cells (K-562, KG1a, and Jurkat) were plated at a density of 1×10^4 cells per well in 96-well plates overnight and then treated with vehicle, different concentrations (1, 10, 25, 50, and 100 μM) of 1,3,4-oxadiazole/chalcone derivatives, **8a-x,** or cisplatin (positive control). After 24 h treatment, 20 μL of MTT solution (2 mg/mL in phosphate-buffered saline [PBS]) was added to each well and the cells were cultured for another 4 h at 37 °C. The medium was aspirated and 150 μL DMSO was added to solubilize MTT formazan crystals. The plates were then shaken, and the optical density was determined at 570 nm using an ELISA plate reader (Model 550, Bio-Rad, USA). At least three independent experiments were performed. The IC_{50} values were calculated using GraphPad Prism 5 (Version 5.01, GraphPad Software, San Diego, CA, USA)

4.2.4. EGFR and Src kinase assay [71]

The EGFR and c-Src kinase assays were carried out in 96-well plates coated with PGT (poly L-glutamic acid L-tyrosine, 4:1, Sigma Aldrich, MO, USA) and incubated at 37 °C for 48 h. PGT acts as the substrate for phosphorylation by EGFR and c-Src (Enzo Life Sciences Inc, NY, USA) in the presence of ATP (50 μM). Different concentrations (0.01, 0.1, 1, 10, and 100 μM) of 1,3,4-oxadiazole/chalcone derivatives (**8a-x**), gefitinib, or dasatinib were added to compete with ATP for binding to ATP-binding site in the kinase domain of EGFR or c-Src. Fifteen ng of EGFR (20 μg/mL) or 6 ng of c-Src (0.1 μg/μL) were added to each well. HRP-conjugated anti-phosphotyrosine antibody (Cell Signaling Technology, Japan) was then used to detect the phosphorylated substrate. The signal was developed by the addition of 3, 3′, 5, 5′-tetramethylbenzidine peroxidase substrate (Abcam, Japan) and the colorimetric reaction was monitored at 450 nm using a microplate reader (Bio-Rad, USA). IC_{50} values were calculated using GraphPad Prism 5. Each experiment was carried out at least three times.

4.2.5. Western blot analysis [72]

K562 cells were incubated with different concentrations of compound **8v** (0.2 μM, 0.8 μM and 1.6 μM), or DMSO 24 h. The protein was then collected and measured. For western blot analysis, 50 μg of protein was loaded onto a 8 or 10% SDS-PAGE gel. Proteins separated on the SDS-PAGE gel were transferred to a polyvinylidene fluoride (PVDF) membrane. The PVDF membrane was incubated in a blocking buffer containing 3% non-fat milk powder, 1% BSA (Sigma-Aldrich), and 0.5% Tween-20 in PBS for 1 h. Subsequently, the PVDF membrane was incubated with the suitable and validated primary antibody (Cell Signaling Technology, Danvers, MA, USA) overnight, followed by horseradish peroxidase (HRP)-conjugated IgG (Cell Signaling Technology, Beverly, MA, USA) for 1 h with gentle agitation at room temperature. Detection was carried out using enhanced chemiluminescence (ECL) prime (GE Healthcare, Little Chalfont, UK) and autoradiography with an X-ray film (Konica Minolta Medical Imaging, Wayne, NJ, USA)

4.2.6. Il-6 ELISA [73]

IL-6 cytokine levels in cell-free culture supernatants were determined using Hu-IL6 Cytoset ELISA kit (Biosource International Inc. CA, USA) according to the manufacturer's instructions. Briefly, K-562 cells were treated with DMSO, 10 μM 1,3,4-oxadiazole/chalcone derivatives (**8a-x),** or dexamethasone (positive control) for 24 h. Cell-free medium supernatants were collected for quantification of levels of secreted IL-6 protein via ELISA. The results were expressed as percentages relative to the vehicle control and as mean ± SD based on three independent experiments, each done in triplicate. The time course effect of compound **8v** on IL-6 protein expression was carried out by culturing K-562 cells in 12-well plates. The media were changed when **8v** (10 μM) was added to the cells. Media were collected at 0, 1, 4, 8, 12, 24, and 48 h and used for IL-6 determination by ELISA and expressed as mean ± SD based on three independent experiments, each done in triplicate.

4.2.7. STAT3 activation assay [74]

K562 cells were seeded in 10 cm plates overnight and then treated with vehicle, 10 μM 1,3,4-oxadiazole/chalcone derivatives (**8a-x),** or WP1066 (positive control) for 24 h. Cells were collected and nuclear fractions were extracted using a Nuclear Extract Kit (Active Motif, Tokyo, Japan) according to the manufacturer's protocol. Nuclear extracts (20 ug) were used to analyze STAT3 activation using the TransAM STAT3 Activation Assay (Active Motif) according to the manufacturer's protocol. The results were expressed as the mean ± SD based on three independent experiments, each done in triplicate.

4.2.8. Statistical analysis

Data were presented as the means ± standard deviations (SD). Student's *t*-test was performed to determine the statistical significance compared to the vehicle treated control. Statistical significance was defined as $^{*}p < 0.05$ or $^{**}p < 0.005$. Data are representative of three independent experiments.

Acknowledgment

Authors thank the Development Therapeutics Program of the National Cancer Institute, Bethesda, MD, USA, for *in vitro* evaluation of the anticancer activity. Grateful thanks are expressed to Dr. Mohammed Abdel Wahaab, Um Al-Qura University, Saudi Arabia for helping in measuring the NMR data.

Conflicts of Interest

The authors declare no conflicts of interest.

Appendix A. Supplementary material

Supplementary data to this article can be found online at https://doi.org/10.1016/j.bioorg.2018.11.032.

References

[1] C.L. Sawyers, C.T. Denny, O.N. Witte, Leukemia and the disruption of normal hematopoiesis, Cell 64 (1991) 337–350 PMID: 1988151.
[2] T. Farge, E. Saland, F. De Toni, N. Aroua, M. Hosseini, R. Perry, C. Bosc, M. Sugita, L. Stuani, M. Fraisse, Chemotherapy-resistant human acute myeloid leukemia cells are not enriched for leukemic stem cells but require oxidative metabolism, Cancer discovery 7 (2017) 716–735, https://doi.org/10.1158/2159-8290.CD-16-0441.
[3] M. Pallis, J. Turzanski, Y. Higashi, N. Russell, P-glycoprotein in acute myeloid leukaemia: therapeutic implications of its association with both a multidrug-resistant and an apoptosis-resistant phenotype, Leukemia Lymphoma 43 (2002) 1221–1228, https://doi.org/10.1080/10428190290026277.
[4] G. Ghiaur, M. Wroblewski, S. Loges, Acute myelogenous leukemia and its microenvironment: a molecular conversation, Seminars Hematol. 52 (2015) 200–206, https://doi.org/10.1053/j.seminhematol.2015.03.003.
[5] C. Bosc, M.A. Selak, J.-E. Sarry, Resistance is futile: targeting mitochondrial energetics and metabolism to overcome drug resistance in cancer treatment, Cell Metab. 26 (2017) 705–707, https://doi.org/10.1016/j.cmet.2017.10.013.
[6] K.S. Siveen, S. Sikka, R. Surana, X. Dai, J. Zhang, A.P. Kumar, B.K. Tan, G. Sethi, A. Bishayee, Targeting the STAT3 signaling pathway in cancer: role of synthetic and natural inhibitors, Biochimica et Biophysica Acta (BBA)-Reviews Cancer 1845 (2014) 136–154, https://doi.org/10.1016/j.bbcan.2013.12.005.
[7] I. De Kouchkovsky, M. Abdul-Hay, Acute myeloid leukemia: a comprehensive review and update, Blood Cancer J. 6 (2016) (2016) 441–450, https://doi.org/10.1038/bcj.2016.50.
[8] N.N. Bewry, R.R. Nair, M.F. Emmons, D. Boulware, J. Pinilla-Ibarz, L.A. Hazlehurst, Stat3 contributes to resistance toward BCR-ABL inhibitors in a bone marrow microenvironment model of drug resistance, Mol Cancer Ther. 7 (2008) 3169–3175, https://doi.org/10.1158/1535-7163.MCT-08-0314.
[9] J. Zhou, C. Bi, J.V. Janakakumara, S.-C. Liu, W.-J. Chng, K.-G. Tay, L.-F. Poon, Z. Xie, S. Palaniyandi, H. Yu, Enhanced activation of STAT pathways and overexpression of survivin confer resistance to FLT3 inhibitors and could be therapeutic targets in AML, Blood 113 (2009) 4052–4062, https://doi.org/10.1182/blood-2008-05-156422.
[10] M.S. Redell, M.J. Ruiz, T.A. Alonzo, R.B. Gerbing, D.J. Tweardy, Stat3 signaling in acute myeloid leukemia: ligand-dependent and -independent activation and induction of apoptosis by a novel small molecule Stat3 inhibitor, Blood 117 (2011) 5701–5709, https://doi.org/10.1182/blood-2010-04-280123.
[11] R.R. Nair, J.H. Tolentino, L.A. Hazlehurst, Role of STAT3 in transformation and drug resistance in CML, Front. Oncol. 2 (2012) 1–12, https://doi.org/10.3389/fonc.2012.00030.
[12] J.G. Paez, P.A. Jänne, J.C. Lee, S. Tracy, H. Greulich, S. Gabriel, P. Herman, F.J. Kaye, N. Lindeman, T.J. Boggon, EGFR mutations in lung cancer: correlation with clinical response to gefitinib therapy, Science 304 (2004) 1497–1500, https://doi.org/10.1126/science.1099314.
[13] R. Buettner, T. Mesa, A. Vultur, F. Lee, R. Jove, Inhibition of Src family kinases with dasatinib blocks migration and invasion of human melanoma cells, Mol. Cancer Res. 6 (2008) 1766–1774, https://doi.org/10.1158/1541-7786.MCR-08-0169.
[14] T. Tanaka, T. Kishimoto, The biology and medical implications of interleukin-6, Cancer Immunol. Res. 2 (2014) 288–294, https://doi.org/10.1158/2326-6066.CIR-

14-0022.
[15] E. Dijkgraaf, S. Santegoets, A. Reyners, R. Goedemans, M. Wouters, G. Kenter, A. van Erkel, M. van Poelgeest, H. Nijman, J. van der Hoeven, A phase I trial combining carboplatin/doxorubicin with tocilizumab, an anti-IL-6R monoclonal antibody, and interferon-α2b in patients with recurrent epithelial ovarian cancer, Ann. Oncol. 26 (2015) 2141–2149, https://doi.org/10.1093/annonc/mdv309.
[16] N. Normanno, A. Morabito, A. De Luca, M.C. Piccirillo, M. Gallo, M.R. Maiello, F. Perrone, Target-based therapies in breast cancer: current status and future perspectives, Endocrine-Related Cancer 16 (2009) 675–702, https://doi.org/10.1677/ERC-08-0208.
[17] A.Z. Dudek, H. Pang, R.A. Kratzke, G.A. Otterson, L. Hodgson, E.E. Vokes, H.L. Kindler, L.G.B. Cancer, Phase II study of dasatinib in patients with previously treated malignant mesothelioma (cancer and leukemia group B 30601): a brief report, J Thorac Oncol. 7 (2012) 755–759, https://doi.org/10.1097/JTO.0b013e318248242c.
[18] E.B. Haura, T. Tanvetyanon, A. Chiappori, C. Williams, G. Simon, S. Antonia, J. Gray, S. Litschauer, L. Tetteh, A. Neuger, Phase I/II study of the Src inhibitor dasatinib in combination with erlotinib in advanced non–small-cell lung cancer, J Clin Oncol. 28 (2010) 1387–1394, https://doi.org/10.1200/JCO.2009.25.4029.
[19] Y. Lin, X. Wang, H. Jin, EGFR-TKI resistance in NSCLC patients: mechanisms and strategies, Am. J. Cancer Res. 4 (2014) 411–435 PMCID: PMC4163608.
[20] H.-J. Lee, G. Zhuang, Y. Cao, P. Du, H.-J. Kim, J. Settleman, Drug resistance via feedback activation of Stat3 in oncogene-addicted cancer cells, Cancer Cell 26 (2014) 207–221, https://doi.org/10.1016/j.ccr.2014.05.019.
[21] T. Ara, R. Nakata, M.A. Sheard, H. Shimada, R. Buettner, S.G. Groshen, L. Ji, H. Yu, R. Jove, R.C. Seeger, Critical role of STAT3 in IL-6–mediated drug resistance in human neuroblastoma, Cancer Res. 73 (2013) 3852–3864, https://doi.org/10.1158/0008-5472.CAN-12-2353.
[22] J. Lin, W. Shen, J. Xue, J. Sun, X. Zhang, C. Zhang, Novel oxazolo [4, 5-g] quinazolin-2 (1H)-ones: dual inhibitors of EGFR and Src protein tyrosine kinases, Eur. J. Med. Chem. 55 (2012) 39–48.
[23] Z. Cui, S. Chen, Y. Wang, C. Gao, Y. Chen, C. Tan, Y. Jiang, Design, synthesis and evaluation of azaacridine derivatives as dual-target EGFR and Src kinase inhibitors for antitumor treatment, Eur. J. Med. Chem. 136 (2017) 372–381.
[24] L. Huang, L. Fu, Mechanisms of resistance to EGFR tyrosine kinase inhibitors, Acta Pharm. Sin B. 5 (2015) 390–401, https://doi.org/10.1016/j.apsb.2015.07.001.
[25] S.P. Gao, K.G. Mark, K. Leslie, W. Pao, N. Motoi, W.L. Gerald, W.D. Travis, W. Bornmann, D. Veach, B. Clarkson, Mutations in the EGFR kinase domain mediate STAT3 activation via IL-6 production in human lung adenocarcinomas, J. Clin. Invest. 117 (2007) 3846–3856, https://doi.org/10.1172/JCI31871.
[26] A. Xiong, Z. Yang, Y. Shen, J. Zhou, Q. Shen, Transcription factor STAT3 as a novel molecular target for cancer prevention, Cancers 6 (2014) 926–957, https://doi.org/10.3390/cancers6020926.
[27] J. Sun, J.A. Makawana, H.-L. Zhu, 1, 3, 4-oxadiazole derivatives as potential biological agents, Mini. Rev. Med. Chem. 13 (2013) 1725–1743 PMID: 23815585.
[28] I. Rasool, M. Ahmad, Z.A. Khan, A. Mansha, T. Maqbool, A.F. Zahoor, S. Aslam, Recent advancements in oxadiazole-based anticancer agents, Trop. J. Pharm. Res. 16 (2017) 723–733, https://doi.org/10.4314/tjpr.v16i3.30.
[29] I. Khan, A. Ibrar, N. Abbas, Oxadiazoles as privileged motifs for promising anticancer leads: recent advances and future prospects, Arch. Pharm. Chem. Life Sci. 347 (2014) 1–20, https://doi.org/10.1002/ardp.201300231.
[30] S. Bajaj, V. Asati, J. Singh, P.P. Roy, 1,3,4-Oxadiazoles: An emerging scaffold to target growth factors, enzymes and kinases as anticancer agents, Eur. J. Med. Chem. 97 (2015) 124–141.
[31] R.N. Kumar, Y. Poornachandra, P. Nagender, G.S. Kumar, D.K. Swaroop, C.G. Kumar, B. Narsaiah, Synthesis of novel nicotinohydrazide and (1,3,4-oxadiazol-2-yl)-6-(trifluoromethyl)pyridine derivatives as potential anticancer agents, Bioorg. Med. Chem. Lett. 26 (2016) 4829–4831.
[32] N. Polkam, B. Kummari, P. Rayam, U. Brahma, V.G.M. Naidu, S. Balasubramanian, J.S. Anireddy, Synthesis of 2,5-disubstituted-1,3,4-oxadiazole derivatives and their evaluation as anticancer and antimycobacterial agents, ChemistrySelect 2 (2017) 5492–5496.
[33] A. Özdemir, B. Sever, M.D. Altıntop, H.E. Temel, Ö. Atlı, M. Baysal, F. Demirci, Synthesis and evaluation of new oxadiazole, thiadiazole, and triazole derivatives as potential anticancer agents targeting MMP-9, Molecules 22 (2017) 1109–1123.
[34] M.J. Ahsan, R.P. Yadav, S. Saini, M.Z. Hassan, M.A. Bakht, S.S. Jadav, A.B.S. Al-Tamimi, M.H. Geesi, M.Y. Ansari, H. Khalilullah, Y. Riadi, Synthesis, cytotoxic evaluation, and molecular docking studies of new oxadiazole analogues, Lett. Org. Chem. 15 (2018) 49–56, https://doi.org/10.2174/1570178614666170704103315.
[35] C.D. Mohan, N.C. Anilkumar, S. Rangappa, M.K. Shanmugam, S. Mishra, A. Chinnathambi, S.A. Alharbi, A. Bhattacharjee, G. Sethi, A.P. Kumar, K.S. Basappa, Rangappa, novel 1,3,4-oxadiazole induces anticancer activity by targeting nF-κB in hepatocellular carcinoma cells, Front Oncol. 8 (2018) 1–11, https://doi.org/10.3389/fonc.2018.00042.
[36] R. Hamdy, N.I. Ziedan, S. Ali, C. Bordoni, M. El-Sadek, E. Lashin, A. Brancale, A.T. Jones, A.D. Westwell, Synthesis and evaluation of 5-(1H-indol-3-yl)-N-aryl-1,3,4-oxadiazol-2-amines as Bcl-2 inhibitory anticancer agents, Bioorg. Med. Chem. Lett. 27 (2017) 1037–1040.
[37] F.A.F. Ragab, S.M. Abou-Seri, S.A. Abdel-Aziz, A.M. Alfayomy, Design, synthesis and anticancer activity of new monastrol analogues bearing 1,3,4-oxadiazole moiety, Eur. J. Med. Chem. 138 (2017) 140–151.
[38] M.T. Javid, F. Rahim, M. Taha, M. Nawaz, A. Wadood, M. Ali, A. Mosaddik, S.A.A. Shah, R.K. Farooq, Synthesis, SAR elucidations and molecular docking study of newly designed isatin based oxadiazole analogs as potent inhibitors of thymidine phosphorylase, Bioorg. Chem. 79 (2018) 323–333.
[39] S. Bajaj, P.P. Roy, J. Singh, Synthesis, thymidine phosphorylase inhibitory and computational study of novel 1,3,4-oxadiazole-2-thione derivatives as potential anticancer agents, Comput. Biol. Chem. 76 (2018) 151–160, https://doi.org/10.1016/j.compbiolchem.2018.05.013.
[40] D. Masciocchi, S. Villa, F. Meneghetti, A. Pedretti, D. Barlocco, L. Legnani, L. Toma, B.-M. Kwon, S. Nakano, A. Asaid, A. Gelain, Biological and computational evaluation of an oxadiazole derivative (MD77) as a new lead for direct STAT3 inhibitors, Med. Chem. Commun. 3 (2012) 592–599, https://doi.org/10.1039/c2md20018j.
[41] S.M. Abou-Seri, Synthesis and biological evaluation of novel 2,4-bis substituted diphenylamines as anticancer agents and potential epidermal growth factor receptor tyrosine kinase inhibitors, Eur. J. Med. Chem. 45 (2010) 4113–4121.
[42] M.J. Akhtar, A.A. Siddiqui, A.A. Khan, Z. Ali, R.P. Dewangan, S. Pasha, M.S. Yar, Design, synthesis, docking and QSAR study of substituted benzimidazole linked oxadiazole as cytotoxic agents, EGFR and erbB2 receptor inhibitors, Eur. J. Med. Chem. 126 (2017) 853–869.
[43] J.-F. Tang, X.-H. Lv, X.-L. Wanga, J. Sun, Y.-B. Zhang, Y.-S. Yang, H.-B. Gong, H.-L. Zhu, Design, synthesis, biological evaluation and molecular modeling of novel 1,3,4-oxadiazole derivatives based on Vanillic acid as potential immunosuppressive agents, Bioorg. Med. Chem. 20 (2012) 4226–4236.
[44] A. Kilimnik, M.N. Kostjukova, I.H. Pyatkin, A.M. Pronin, S.R.S. Trelnikova, Y.A. Fedotov, A.V. Kolesnikov, Novel small-molecule inhibitors of C-terminal Src kinase (Csk), Cell Mol Biol. Lett. 8 (2003) 588–589.
[45] A. Lavecchia, C. Di Giovanni, C. Cerchia, Novel inhibitors of signal transducer and activator of transcription 3 signaling pathway: an update on the recent patent literature, Expert Opin. Ther. Pat. 24 (2014) 383–400, https://doi.org/10.1517/13543776.2014.877443.
[46] D.K. Mahapatra, S.K. Bharti, V. Asati, Anti-cancer chalcones: Structural and molecular target perspectives, Eur. J. Med. Chem. 98 (2015) 69–114.
[47] E.B. Yang, Y.J. Guo, K. Zhang, Y.Z. Chen, P. Mack, Inhibition of epidermal growth factor receptor tyrosine kinase by chalcone derivatives, Biochim. Biophys. Acta. 1550 (2001) 144–152 PMID: 11755203.
[48] L. Chen, W. Fu, L. Zheng, Z. Liu, G. Liang, Recent progress of small-molecule epidermal growth factor receptor (EGFR) Inhibitors against C797S resistance in non-small-cell lung cancer, J. Med. Chem. 61 (2018) 4290–4300.
[49] K. Chand, A.N. Shirazi, P. Yadav, R.K. Tiwari, M. Kumari, K. Parang, S.K. Sharma, Synthesis and antiproliferative and c-Src kinase inhibitory activities of cinnamoyl- and pyranochromen-2-one derivatives, Can. J. Chem. 91 (2013) 741–754, https://doi.org/10.1139/cjc-2013-0053.
[50] I. Jantan, S.N.A. Bukhari, O.A. Adekoya, I. Sylte, Studies of synthetic chalcone derivatives as potential inhibitors of secretory phospholipase A2, cyclooxygenases, lipoxygenase and pro-inflammatory cytokines, Drug Des. Devel. Ther. 8 (2014) 1405–1418, https://doi.org/10.2147/DDDT.S67370.
[51] F.F. Ahmed, A.A. Abd El-Hafeez, S.H. Abbas, Dalia Abdelhamid, Mohamed Abdel-Aziz, New 1,2,4-triazole-Chalcone hybrids induce Caspase-3 dependent apoptosis in A549 human lung adenocarcinoma cells, Eur. J. Med. Chem. 151 (2018) 705–722.
[52] A. Novilla, M. Mustofa, I. Astuti, J. Jumina, H. Suwito, Molecular mechanism of synthesized chalcone as an anticancer agent in Leukemia Cell Line HL60, Biosci. Res. 14 (2017) 731–740.
[53] P. Rajendran, T.H. Ong, L. Chen, F. Li, M.K. Shanmugam, S. Vali, T. Abbasi, S. Kapoor, A. Sharma, A.P. Kumar, K.M. Hui, G. Sethi, Suppression of signal transducer and activator of transcription 3 Activation by butein inhibits growth of human hepatocellular carcinoma in vivo, Clin. Cancer Res. 17 (2011) 1425–1439, https://doi.org/10.1158/1078-0432.CCR-10-1123.
[54] J. Zhang, S. Sikka, K.S. Siveen, J.H. Lee, J.-Y. Um, A.P. Kumar, A. Chinnathambi, S.A. Alharbi, Basappa, K.S. Rangappa, G. Sethi, K.S. Ahn, Cardamonin represses proliferation, invasion, and causes apoptosis through the modulation of signal transducer and activator of transcription 3 pathway in prostate cancer, Apoptosis 22 (2017) 158–168, https://doi.org/10.1007/s10495-016-1313-7.
[55] C. Bagul, G.K. Rao, V.K.K. Makani, J.R. Tamboli, M. Pal-Bhadra, A. Kamal, Synthesis and biological evaluation of chalcone linked pyrazolo[1,5-a]pyrimidines as potential anticancer agents, Med. Chem. Commun. 8 (2017) 1810–1816, https://doi.org/10.1039/C7MD00193B.
[56] M.J. Mphahlele, M.M. Maluleka, N. Parbhoo, S.T. Malindisa, Synthesis, evaluation for cytotoxicity and molecular docking studies of benzo[c]furan-chalcones for potential to inhibit tubulin polymerization and/or EGFR-tyrosine kinase phosphorylation, Int. J. Mol. Sci. 19 (2018) 2552–2569, https://doi.org/10.3390/ijms19092552.
[57] M. Alswah, A.H. Bayoumi, K. Elgamal, A. Elmorsy, S. Ihmaid, H.E.A. Ahmed, Design, synthesis and cytotoxic evaluation of novel chalcone derivatives bearing triazolo[4,3-a]-quinoxaline moieties as potent anticancer agents with dual EGFR kinase and tubulin polymerization inhibitory effects, Molecules 23 (2018) 48–53.
[58] S.S. Chhajed, S.S. Sonawane, C.D. Upasani, S.J. Kshirsagar, P.P. Gupta, Design, synthesis and molecular modeling studies of few chalcone analogues of benzimidazole for epidermal growth factor receptor inhibitor in search of useful anticancer agent, Comput. Biol. Chem. 61 (2016) 138–144, https://doi.org/10.1016/j.compbiolchem.2016.02.001.
[59] M. Abdel-Aziz, S.-E. Park, G.E.-D.A.A. Abuo-Rahma, M.A. Sayed, Y. Kwon, Novel *N*-4-piperazinyl-ciprofloxacin-chalcone hybrids: synthesis, physicochemical properties, anticancer and topoisomerase I and II inhibitory activity, Eur. J. Med. Chem. 69 (2013) 427–438.
[60] H. Shi, Y. Wang, R. Hua, Acid-catalyzed carboxylic acid esterification and ester hydrolysis mechanism: acylium ion as a sharing active intermediate via a spontaneous trimolecular reaction based on density functional theory calculation and supported by electrospray ionization-mass spectrometry, Phys. Chem. Chem. Phys. 17 (2015) 30279–30291, https://doi.org/10.1039/c5cp02914g.
[61] X. Zhang, M. Breslav, J. Grimm, K. Guan, A. Huang, F. Liu, C.A. Maryanoff, D. Palmer, M. Patel, Y. Qian, C. Shaw, K. Sorgi, S. Stefanick, D. Xu, A new procedure

for preparation of carboxylic acid hydrazides, J. Org. Chem. 67 (2002) 9471–9474 PMID: 12492358.
[62] J.R. Maxwell, D.A. Wasdahl, A.C. Wolfson, V.I. Stenberg, Synthesis of 5-aryl-2*H*-tetrazoles, 5-aryl-2*H*-tetrazole-2-acetic acids, and [(4-phenyl-5-aryl-4*H*-1,2,4-triazol-3-yl)thio]acetic acids as possible superoxide scavengers and antiinflammatory agents, J. Med. Chem. 27 (1984) 1565–1570.
[63] H. He, W. Wang, Y. Zhou, Q. Xia, Y. Ren, J. Feng, H. Peng, H. He, L. Feng, Rational design, synthesis and biological evaluation of 1,3,4-oxadiazole pyrimidine derivatives as novel pyruvate dehydrogenase complex E1 inhibitors, Bioorg. Med. Chem. 24 (2016) 1879–1888.
[64] A.S. Aboraia, H.M. Abdel-Rahman, N.M. Mahfouz, M.A. EL-Gendy, Novel 5-(2-hydroxyphenyl)-3-substituted-2,3-dihydro-1,3,4-oxadiazole-2-thione derivatives: Promising anticancer agents, Bioorg. Med. Chem. 14 (2006) 1236–1246.
[65] D.A. Charistos, G.V. Vagenas, L.C. Tzavellas, C.A. Tsoleridis, N.A. Rodios, Synthesis and a UV and IR spectral study of some 2-aryl-Δ^{2}-1,3,4-oxadiazoline-5-thiones, J. Heterocycl. Chem. 31 (1994) 1593–1598, https://doi.org/10.1002/jhet.5570310653.
[66] H.S. Abd-Ellah, M. Abdel-Aziz, M.E. Shoman, E.A.M. Beshr, T.S. Kaoud, A.-S.F.F. Ahmed, Novel 1,3,4-oxadiazole/oxime hybrids: synthesis, docking studies and investigation of anti-inflammatory, ulcerogenic liability and analgesic activities, Bioorg. Chem. 69 (2016) 48–63.
[67] C.-J. Chen, B.-A. Song, S. Yang, G.-F. Xu, P.S. Bhadury, L.-H. Jin, D.-Y. Hu, Q.-Z. Li, F. Liu, W. Xue, P. Lu, Z. Chen, Synthesis and antifungal activities of 5-(3,4,5-Trimethoxyphenyl)-2-sulfonyl-1,3,4-thiadiazole and 5-(3,4,5-trimethoxyphenyl)-2-sulfonyl-1,3,4-oxadiazole derivatives, Bioorg. Med. Chem. 15 (2007) 3981–3989.
[68] M.A.E. Mourad, M. Abdel-Aziz, G.E.-D.A.A. Abuo-Rahma, H.H. Farag, Design, synthesis and anticancer activity of nitric oxide donating/chalcone hybrids, Eur. J. Med. Chem. 54 (2012) 907–913.
[69] J.-P. Magaud, I. Sargent, D.Y. Mason, Detection of human white cell proliferative responses by immunoenzymatic measurement of bromodeoxyuridine uptake, J. Immunol. Methods 106 (1988) 95–100 PMID: 3276790.
[70] J. van Meerloo, G.J. Kaspers, J. Cloos, Cell sensitivity assays: the MTT assay, Methods Mol Biol. 731 (2011) 237–245, https://doi.org/10.1007/978-1-61779-080-5_20.
[71] S. Rao, A.-L. Larroque-Lombard, L. Peyrard, C. Thauvin, Z. Rachid, C. Williams, B.J. Jean-Claude, Target modulation by a kinase inhibitor engineered to induce a tandem blockade of the epidermal growth factor receptor (EGFR) and c-Src: the concept of type III combi-targeting, PloS one 10 (2015) 1–24, https://doi.org/10.1371/journal.pone.0117215.
[72] A.A. Abd El-Hafeez, H.O. Khalifa, R.A. Elgawish, S.A. Shouman, M.H. El-Twab, S. Kawamoto, Melilotus indicus extract induces apoptosis in hepatocellular carcinoma cells via a mechanism involving mitochondria-mediated pathways, Cytotechnology 70 (2018) 831–842, https://doi.org/10.1007/s10616-018-0195-7.
[73] H. Xu, D. Dinsdale, B. Nemery, P.H. Hoet, Role of residual additives in the cytotoxicity and cytokine release caused by polyvinyl chloride particles in pulmonary cell cultures, Toxicol. Sci. 72 (1) (2003) 92–102 PMID: 12604838.
[74] C. Agarwal, A. Tyagi, M. Kaur, R. Agarwal, Silibinin inhibits constitutive activation of Stat3, and causes caspase activation and apoptotic death of human prostate carcinoma DU145 cells, Carcinogenesis 28 (2007) 1463–1470, https://doi.org/10.1093/carcin/bgm042.